Numerical study of the ocean circulation on the East China Sea shelf and a Kuroshio bottom branch northeast of Taiwan in summer

Dezhou Yang,[1,2] Baoshu Yin,[1] Zhiliang Liu,[1] and Xingru Feng[1,2]

Received 28 October 2010; revised 24 February 2011; accepted 9 March 2011; published 24 May 2011.

[1] Using the Regional Ocean Model System, the ocean circulation on the East China Sea (ECS) shelf was examined by a fine-resolution model which was nested in a coarse-resolution Pacific Ocean model. The high-resolution simulation shows an accurate volume transport of 2.70 Sv (Sv ≡ 10^6 m^3s^{-1}) through the Tsushima Strait, which is more consistent with the previous 5.5 year observation value (2.64 Sv) than former model results. For the Taiwan Strait it also shows a close volume transport (1.03 Sv) to a recent estimate (1.20 Sv). At the same time the model results reproduced almost all of the known circulation structure on the ECS shelf. In addition, the hindcast of 2009 shows a Kuroshio Bottom Branch Current to the northeast of Taiwan (KBBCNT). The KBBCNT is confirmed by the observational bottom high-salinity water (from 15 August to 2 September 2009) whose distribution is also reproduced by the model results. Tracer and particle experiments were carried out to elucidate the formation of the high-salinity water and the pathway of the KBBCNT. In light of the field observation and numerical experiments, a new pathway of the KBBCNT is proposed: bifurcated from the subsurface water of Kuroshio northeast of Taiwan, it upwells northwestward gradually from 300 to 60 m, then turns to northeast in the region around 27.5°N, 122°E, and finally reaches 31°N off the mouth of the Changjiang River along ~60 m isobaths, forming the bottom saline water off the coast of Zhejiang province, China.

Citation: Yang, D., B. Yin, Z. Liu, and X. Feng (2011), Numerical study of the ocean circulation on the East China Sea shelf and a Kuroshio bottom branch northeast of Taiwan in summer, *J. Geophys. Res.*, *116*, C05015, doi:10.1029/2010JC006777.

1. Introduction

[2] The East China Sea (ECS) continental shelf is an extremely dynamic oceanic region which is influenced by the South China Sea (SCS) water passing through the Taiwan Strait (TS), the Yellow Seawater by the China Coast Current (CCC), the Changjiang River, one of the biggest rivers by discharge volume in the world, and Kuroshio, the western boundary current of the North Pacific subtropical gyre. The Kuroshio is considered to enter the ECS through the so-called East Taiwan Channel between Taiwan and Yonaguni-jima Island (YJI; see Figure 1) which lies 108 km from the east coast of Taiwan and is the southernmost one of the Ryukyu Islands chain. Under the constraint of the steep ECS continental slope, the mainstream of the Kuroshio in the ECS runs stably along the 200 m isobath at a maximum velocity of 0.75–1.5 m s^{-1} [*Nitanni*, 1972]. Passing through the Okinawa Trough, the Kuroshio hugs the shelf break of the ECS until it approaches the shoaling northern end of the trough, where it separates from the shelf and bends east–southeastward. After it turns eastward around 30°29′N latitude and 129°E longitude [*Qiu and Imasato*, 1990], the Kuroshio separates from the continental margin, and eventually flows into the Pacific Ocean through the Tokara Strait. The Kuroshio influences not only global ocean climate variations but also the regional ocean system on the ECS continental shelf. The ECS circulation pattern is largely controlled by the Kuroshio which influences the water and heat exchanges of the ECS with the open sea. Therefore, it is a key point in modeling the ECS ocean circulation that the regional ocean model is capable of reproducing the major characteristics of the Kuroshio. However, the results of a local marginal sea model depend closely on the artificial boundary conditions along the open boundary, where the vertical structures of current as well as their temporal variations are usually unknown [*Guo et al.*, 2003, 2006].

[3] According to methods dealing with the open boundary, numerical simulation studies of ocean circulation on the ECS continental shelf are categorized into two categories: (1) open boundary conditions (temperature, salinity, volume transport, etc.) are prescribed in line with the observed values while the open boundaries without observation are set to be artificial sidewall [*Chang and Isobe*, 2003; *Lee and Chao*, 2003; *Lee and Matsuno*, 2007; *Kako et al.*, 2010]; and (2) open

[1]Key Laboratory of Ocean Circulation and Waves, Institute of Oceanology, Chinese Academy of Sciences, Qingdao, China.
[2]Graduate School, Chinese Academy of Sciences, Beijing, China.

0148-0227/11/2010JC006777

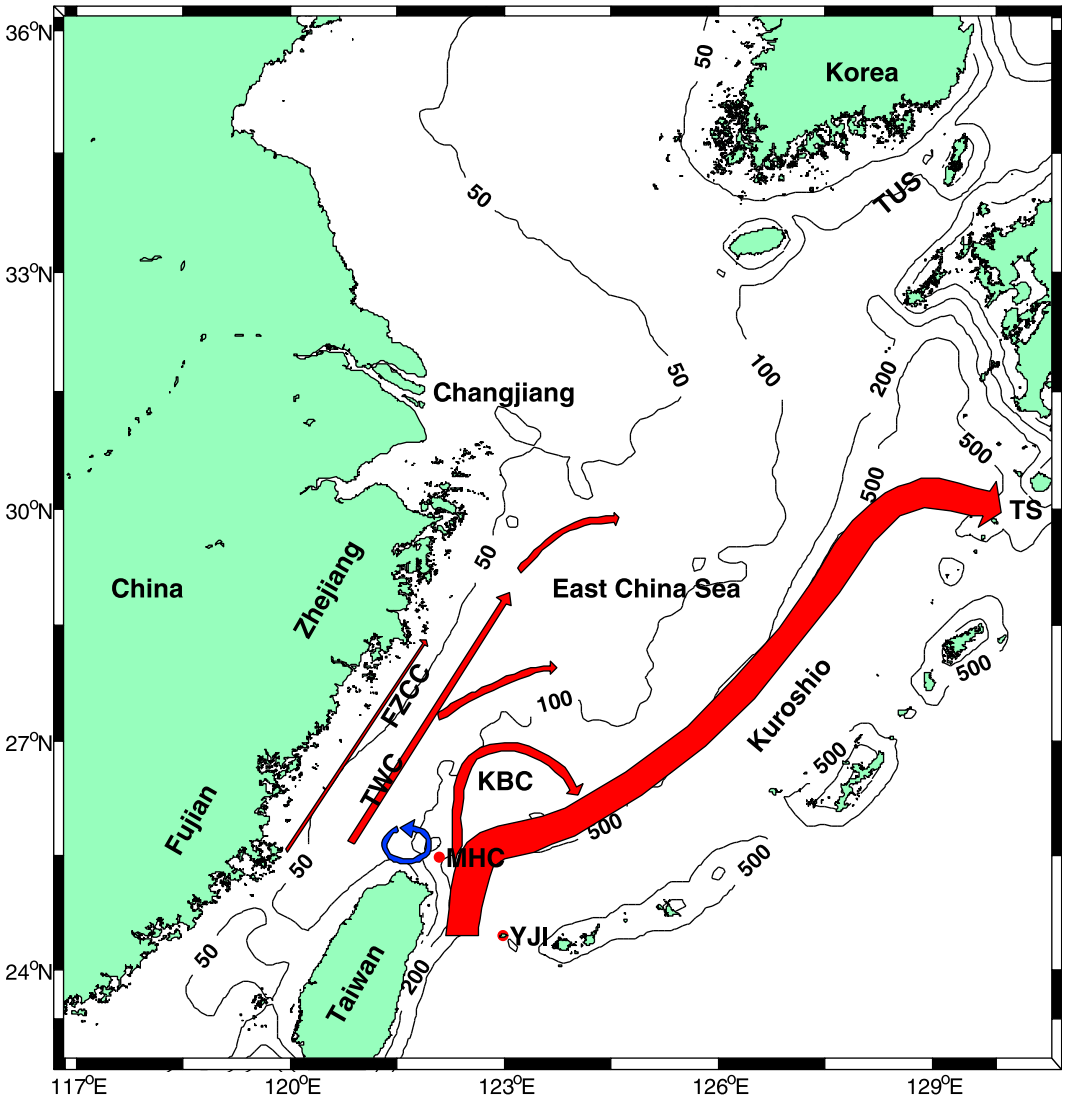

Figure 1. Bottom topography and schematic of summer circulation pattern in the southern ECS. The 50, 100, 200, and 500 m isobaths are shown. YJI, Yonaguni-jima Island; MHC, Mien Hwa Canyon; TWC, Taiwan Warm Current; FZCC, Fujian Zhejiang Coast Current, which flows southward in winter [*Guan and Fang*, 2006]; and KBC, Kuroshio Branch Current [*Qiu and Imasato*, 1990].

boundary conditions are provided by coarse-grid global model or basin-scale ocean model [*Guo et al.*, 2003, 2006; *Wu et al.*, 2008]. In the first category, high-resolution data both in space and time along the open boundaries are frequently unavailable, because the range of open boundary is too large to be surveyed continuously. However, artificial sidewall will influence the water and heat exchanges between open sea and model domain, and it, in turn, will change the circulation pattern there. Only a global ocean model could avoid the problem of open boundary conditions but the computer resources limit its resolution, which is crucial to resolving the shelf break of the ECS [*Guo et al.*, 2003]. A nested model can be a solution to the dilemma between model resolution and model domain. One of the most notable works in the second category has been done by *Guo et al.* [2003]. Using the one-way nested method, *Guo et al.* [2003] have developed a triply nested prognostic model with 1/18° (~6 km) horizontal resolution for the eastern Asian marginal seas covering the ECS, which is nested in a 1/6° horizontal-resolution model whose boundary conditions are derived from a coarse-resolution (1/2°) Pacific Ocean model. *Guo et al.* [2003] suggest that a numerical model needs to have a grid size less than 10 km to simulate correctly the Kuroshio pattern because the continental slope in the ECS has a gradient of as much as 800 m in 20–30 km. The 1/18° horizontal-resolution model of Guo shows relatively accurate Taiwan Warm Current (TWC) and Kuroshio patterns [*Guo et al.*, 2006], although there is a big discrepancy between the modeled volume transport across the Taiwan Strait (TS) 1.71 Sv [*Guo et al.*, 2006] and the recent value 1.20 Sv [*Isobe*, 2008]. In addition, there is an overshooting of Kuroshio Extension in the results of *Guo et al.* [2003, Figure 6] which may be caused by his coarse resolution (1/2°, ~54 km) of Pacific Ocean model. As reported by *Hasumi et al.* [2010], a horizontal grid size of 20 km at ~30°N is a threshold to its proper representation. Therefore in this paper, the resolution

(1/6° × 1/6°cosφ, ~16 km at ~30°N) was used in the whole Pacific Ocean to produce accurate boundary conditions for the ECS numerical simulation, while the fine resolution (1/12° × 1/12°cosφ, ~8 km) was used in the ECS.

[4] Despite recent progresses in observational oceanography and numerical simulation studies, the Kuroshio Branch Current to the northeast of Taiwan (KBCNT) (especially the intrusion path of the KBCNT in the deep and bottom water on the ECS shelf) is still a question of debate [*Isobe*, 2008]. Off the northeastern coast of Taiwan, the northeastward Kuroshio is blocked by steep, north-south running breaks of the ECS and then separated into two parts: the mainstream and its branch [*Kondo*, 1985; *Tang et al.*, 2000], the KBCNT. As regards the existence and pathway of the KBCNT, there are different opinions among scientists.

[5] Some scientists [*Guan*, 1978, 1994, 2002; *Guan and Mao*, 1982; *Fang et al.*, 1991; *Su et al.*, 1994; *Guo et al.*, 2004] favor the ECS circulation schematic in summer where the KBCNT cannot be found in the southern ECS which is mainly occupied by the Taiwan Warm Current (TWC; see Figure 1). The TWC was initially proposed as an independent current in the ECS by Guan in 1964 [*Guan*, 1978]. In summer, the TWC flows to the NNE in the longitudinal direction of the TS off Fujian-Zhejiang coast with a stronger speed of about 20–40 cm s^{-1}, and turns to the ENE off the mouth of the Changjiang River with a weaker speed of about 10 cm s^{-1}; in addition, between the TWC and Kuroshio, there are weak (~10 cm s^{-1}) northeastward offshoot currents which are continuously separated from mainstream of TWC north of 28°N [*Guan and Fang*, 2006]. As to the TWC north of 28°N, *Su and Pan* [1987] proposed that near the 28°N, the TWC bifurcates into two branches: inshore branch (TWCIB, this is the traditional TWC) which flows northward and turns to the northeast off the mouth of the Changjiang River, and offshore branch (TWCOB) which first flows anticyclonically, then turns cyclonically and finally joins the western flank of the Kuroshio. In addition, it is noteworthy that the TWC is considered as a part of the Taiwan-Tsushima-Tsugaru Warm Current System which originates from the Taiwan Strait, flows over the continental shelf of the ECS, intrudes into the East Sea (Japan Sea) through Tsushima Strait, and finally enters the Pacific Ocean through the Tsugaru Strait [*Fang et al.*, 1991].

[6] However, *Kondo* [*Kondo*, 1985] presented schematic diagram of the ECS current system in summer, showing a nearly northward current which is separated from the Kuroshio northeast of Taiwan and flows roughly along the meridian of 124°E to the area about 100 miles east of the Hangzhou Bay. This current is called the KBCNT [see *Ichikawa and Beardsley*, 2002, Figure 6] or "Kuroshio Separation." In addition, a small eastward or northeastward bifurcation may occur from the KBCNT near 28°N. The KBCNT presented by Kondo was based on an analysis of mean distribution of water properties at 50 m depth; its position is farther offshore than that of the TWC. *Qiu and Imasato* [1990] pointed out that the KBCNT does really exist, but the KBCNT has a tendency to turn to ESE near 27°N to rejoin the mainstream of the Kuroshio after it impinges onto the continental shelf north of Taiwan (Figure 1). However, in the schematic representation of the ocean current system in the ECS, *Hishida* [1994] still used almost the same path of KBCNT as Kondo did in 1985. On the basis of current measurements made at two mooring stations in the offshore area north of Taiwan from July 1980 through June 1981, *Chern and Wang* [1989, 1990] found that the Kuroshio Branch Current (KBC; see Figure 1) occurred at depths below 60 m, with speeds of about 10–20 cm s^{-1} in summer, where the water depth is about 120 m. The current flows northwestward along the northern coast of Taiwan and is a major source of the cool, saline water over the shelf of the southwestern ECS, that is, it is the major source of the TWC in deep and bottom layers. The observational results of *Chern and Wang* [1989, 1990] were supported by a two layer numerical circulation model of the ECS by *Liang and Su* [1994], which indicated that the Kuroshio northeast of Taiwan always intruded onto the ECS shelf, but manifested itself chiefly in the lower layer; and after intruding onto the ECS shelf, most of the lower-layer Kuroshio water turned anticyclonically, forming the outer branch of the lower-layer TWC. Therefore, the KBCNT suggested by *Kondo* [1985] does exist, but it appears only in the subsurface layer (below about 60 m depth) and flows northwestward along the north coast of Taiwan rather than straightforwardly along the meridian of 124°E to the offshore area 100 miles away from Hangzhou Bay as *Kondo* [1985] depicted. According to *Ichikawa and Beardsley* [2002, Figure 10], a short KBCNT was marked to the east of the TWC (i.e., the KBCNT north of 29°N did not exist and turned to NE or SE).

[7] Besides the above investigations, the following points of view on the circulation pattern north of Taiwan are worth mentioning. From the 30 m and 100 m isobaths vector maps of composite current velocity which were measured by Shipboard Acoustic Doppler Current Profiler (Sb-ADCP) during 1991–2000 [*Liang et al.*, 2003, Figure 4], it can be easily found that there is a northwestward flow at the depths of 30 and 100 m in the region around 25.3–25.8°N, 121.7–122.2°E, respectively. At 30 m depth the current goes northward along the meridian of 122.0°E, however at 100 m depth it turns anticyclonically and goes northwestward, intruding onto the southern ECS shelf. Off the mouth of the Changjiang River, in the area of 122°.20′–123°.10′E, 31.00–32.00°N, the Kuroshio subsurface water (KSSW) was found in the deep and bottom layers, and contributed abundant nutrients to the upper water by upwelling [*Zhao et al.*, 2001]. The TWC surface water and Kuroshio surface water are devoid of nutrients, whereas the KSSW are rich in nutrients [*Zhang et al.*, 2007]. Though the KSSW was found in the deep and bottom waters off the mouth of the Changjiang River, the question how the KSSW be carried to that area, has not yet been entirely resolved. Simultaneously, the detailed current distribution of the KBC at a depth of 100–200 m north of Taiwan, is still unknown, although the Kuroshio no doubt intrudes onto the ECS northeast of Taiwan crossing the shelf break of the ECS [*Isobe*, 2008].

[8] Obviously, on the southern ECS shelf, TWC [*Guan*, 1978] and KBCNT [*Kondo*, 1985] seems to be mutually exclusive, otherwise the TWC would be crossed by the KBCNT. Compared with the KBCNT and the TWC, the KBC [*Qiu and Imasato*, 1990, Figure 1] seems to a more reasonable current pattern, but KBC cannot explain the bottom high-salinity water off Zhejiang coast.

[9] A fine-resolution model has been developed for ECS in this paper, and it was used, together with field observation, to investigate the intrusion of KBCNT. This paper is

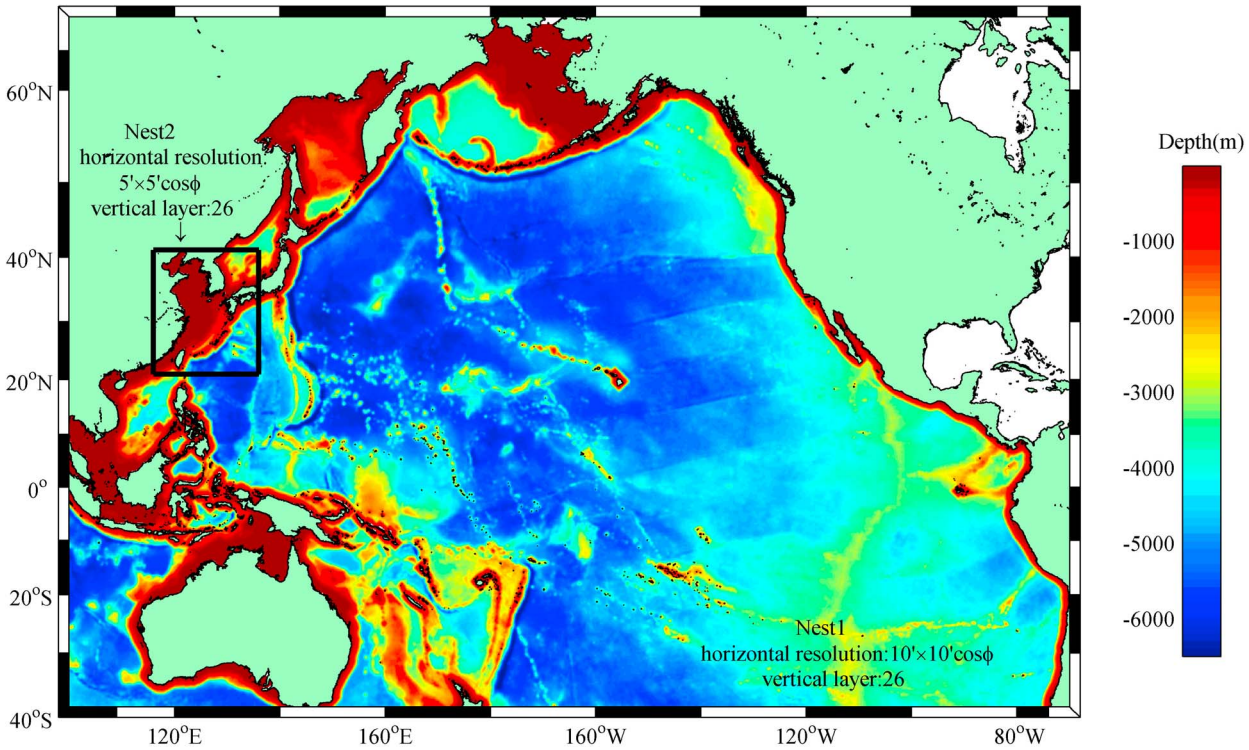

Figure 2. Domains of one-way nested models Nest1 and Nest2. Topography is based on ETOPO5 and ETOPO1.

organized as follows. Model details are provided in section 2. Model results and comparison with observation are shown in section 3. In section 4, numerical experiments, together with observation data analysis, were conducted to investigate the bottom branch of Kuroshio. Section 5 gives the conclusion.

2. Model Descriptions

[10] The ROMS is a three dimensional, free surface, hydrostatic, primitive equation numerical ocean model based on the nonlinear terrain-following coordinate (*s* coordinate) of *Song and Haidvogel* [1994]. The horizontal and vertical diffusions are calculated using the Smagorinsky diffusion parameterization and the KPP scheme [*Large et al.*, 1994], respectively. Details of the ROMS computational algorithms are suggested by *Shchepetkin and McWilliams* [2005].

[11] As to North Pacific modeling, *Hasumi et al.* [2010] pointed out that a horizontal grid size of 20 km at ~30°N is a threshold to the proper representation of Kuroshio Extension and separation. In the modeling of ocean circulation on the ECS shelf, it was reported by *Guo et al.* [2003, 2006] that the model resolution should be less than 10 km to resolve the steep shelf break in the ECS along which the Kuroshio flows. In addition, the model needs to resolve the vertical structure of the Kuroshio because the interaction between topography and baroclinicity is crucial to the cross-isobath currents in the ECS [*Guo et al.*, 2006]. Therefore, to achieve high resolution in the Kuroshio region in Nest1 (Figure 2), we use the 2/1 grid ratio to decrease the grid size from 1/6° × 1/6°cosΦ (~18 km, where Φ is latitude) in Nest1 (98°E–112°W; 40°S–67°N) to 1/12° × 1/12°cosΦ (~8 km) in Nest2 (116°E–136°E; 21°N–41°N). In both models, the model domain is divided into 26 *s* coordinate levels in the vertical, using the same parameters of *s* coordinate [*Song and Haidvogel*, 1994] but Tcline (a positive thickness controlling the stretching of *s* coordinate) which is 5 m in Nest2 and 10 m in Nest1, respectively. The bottom topography is extracted from a combination of two topographic data sets ETOPO5 and ETOPO1 (http://www.ngdc.noaa.gov/mgg/global/). One modification is done to the original topography data: setting the minimum (10 m in Nest1 and 5 m in Nest2) and maximum (6500 m in Nest1 and Nest2) depths.

2.1. Initial Conditions

[12] The climatology monthly mean temperature and salinity in January derived from WOA09 (http://www.nodc.noaa.gov/OC5/WOA09/pubwoa09.html) are used to initialize the Nest1 model. The initial current velocity of Nest1 is set equal to the combination of geostrophical current and Ekman current which are calculated from the temperature and salinity data of WOA09 according to the Sverdrup Theory [*Pedlosky*, 1996]. A correction with respect to surface temperature, dQ/dSST derived from bulk formulas, is used to introduce thermal feedback [*Marchesiello et al.*, 2001]. The Sea Surface Height (SSH) is nudged by the monthly mean SSH fields from the DUACS delayed time product (http://www.aviso.oceanobs.com/duacs/).

2.2. Open Boundary Conditions

[13] Four lateral boundaries of Nest1 are treated as wall for simplicity. This simplicity is acceptable because the boundaries are far away from the Nest2. As for Nest2, the boundary condition is treated in the following manner. First, the depths

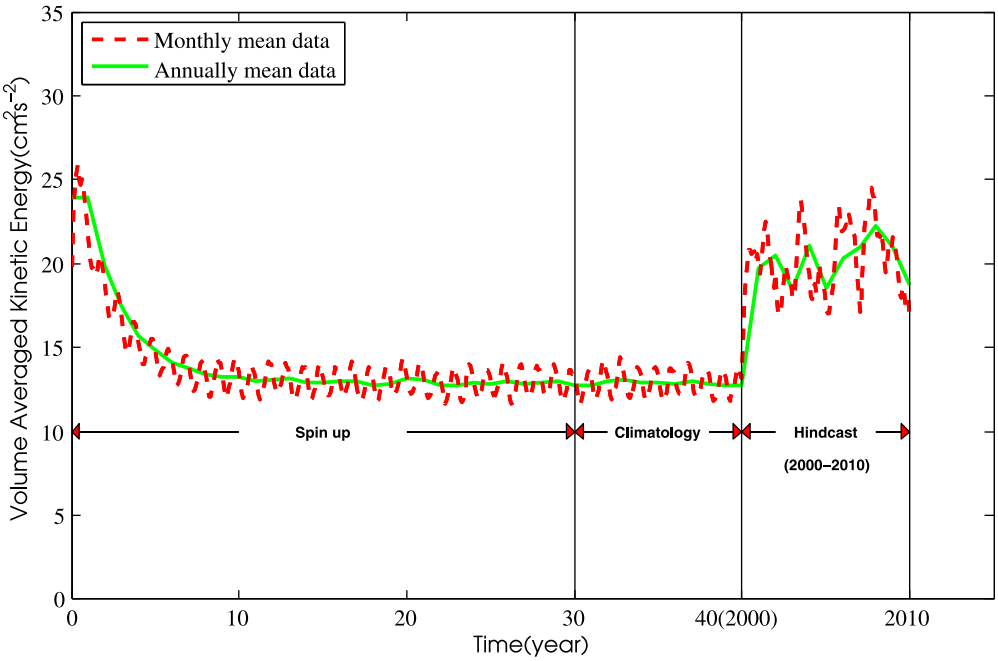

Figure 3. Time evolution of the volume-averaged kinetic energy in Nest1.

of Nest2 along the boundary are set equal to those of Nest1. Next, along the boundaries of Nest2, the unknown variables, that is, elevation, velocity, temperature and salinity, are obtained by spatial (bilinear) interpolation of the Nest1 model results. In addition, before the results of Nest1 model are supplied to Nest2 model, the volume transport is modulated smoothly to guarantee the conservation of volume flux through the open boundaries of Nest2.

[14] Both Nest1 and Nest2 models use the sponge and nudging layers. The values of the sponge and nudging parameters vary as cosine function from a maximum at the boundary to zero at the inner edge of the layer; the layer width is set to 100 km (i.e., on the order of mesoscale structures); and the maximum viscosity/diffusivity values for the sponge layer are set to 100/50 $m^2\ s^{-1}$ on the basis of the results of *Marchesiello et al.* [2001].

2.3. Climatology Runs

[15] For spin-up of Nest1 model, it is integrated for 30 years and forced by monthly mean climatology data varying in time with an annual cycle of 360 days. The climatology data are composed of the monthly mean wind stresses, net heat fluxes, net fresh water fluxes, surface solar shortwave radiation, sea surface temperature (SST), and sea surface salinity (SSS) from COADS [*Diaz et al.*, 2002].

[16] Thereafter, the Nest2 model starts from the initial conditions interpolated from the Nest1 results, is forced by the same surface conditions as Nest1, and is integrated for 10 years for spin-up.

2.4. Hindcast Runs

[17] During hindcast duration from January 2000 to January 2010, Nest1 and Nest2 start from the results of climatology runs, and are forced by the daily mean wind stresses, net heat fluxes, net fresh water fluxes, and surface solar shortwave radiation derived from ERA-interim (http://data-portal.ecmwf.int/data/d/interim_daily). Different to monthly mean forcing data of climatology runs, SST is derived from weekly mean data (http://data.nodc.noaa.gov/pathfinder/), and the SSH is also derived from weekly mean data (http://www.aviso.oceanobs.com/duacs/). In addition to these factors, the daily mean discharges (http://xxfb.hydroinfo.gov.cn) of Changjiang River are added to the models. It is noteworthy that the Nest2 model is also forced by tidal forcing (10 constituents) from the TPXO7 [*Egbert and Erofeeva*, 2002].

[18] These simulations are performed on 768 processors (forty-eight 16 processor nodes) of the massively parallel computer at the High Performance Computational Center, Institute of Oceanology, Chinese Academy of Sciences (IOCAS). Monthly simulations of Nest1 model could usually be performed in 0.5 h.

3. Model Results

[19] Figure 3 depicts the time evolution of volume-integrated kinetic energy (KE) for the entire volume in Nest1 model. The volume-integrated KE shows a clear seasonal cycle, while it exhibits interannual variability as a consequence of the intrinsic variability owing to mesoscale instability of the seasonally forced currents. After a spin-up period of about 30 years, the volume-integrated KE has a tendency to oscillate slowly around an equilibrium value. The volume-integrated KE of hindcast of (2000–2010) is larger than that of climatology run, because the climatology forcing data is smoothed over a period of one month.

3.1. Circulation Pattern and Volume Transports

[20] Figure 4 shows the monthly mean current distributions at the 20 m depth in August and February, the tenth year of climatology run of Nest2. These current distributions are typical summer (Figure 4a) and winter (Figure 4b) circulation

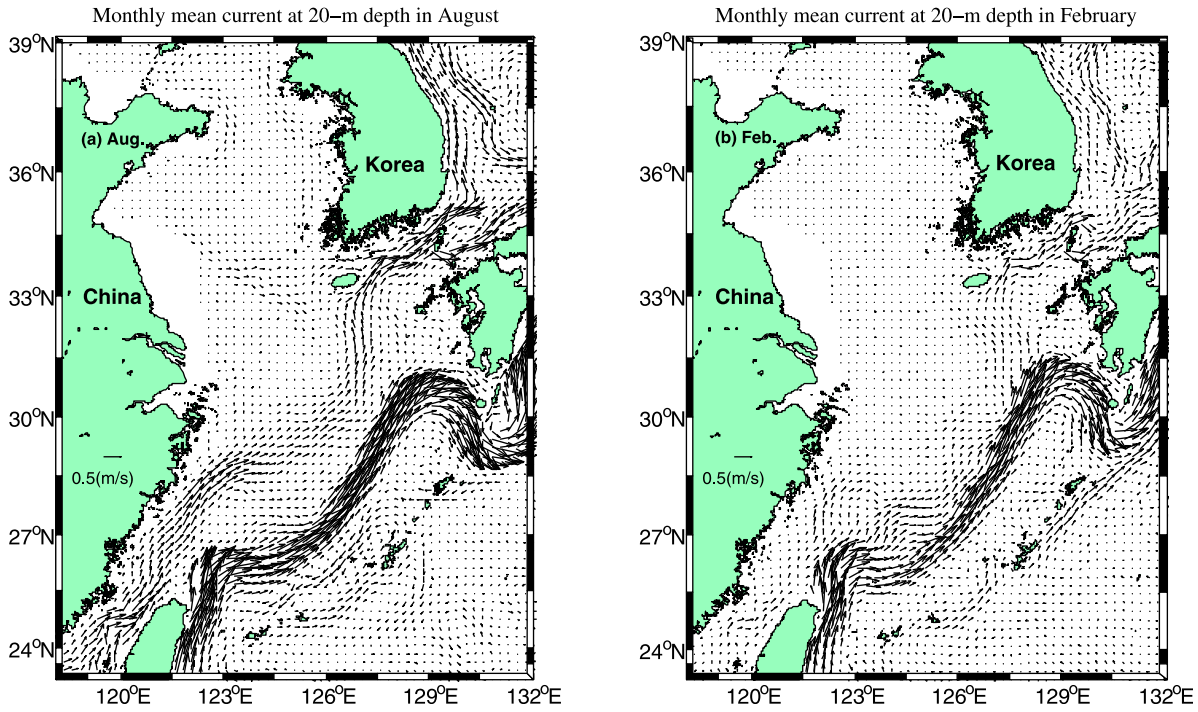

Figure 4. Monthly mean surface current distribution at 20 m depth in (a) August and (b) February.

patterns which mirror the findings of *Guan* [1978] and *Qiu and Imasato* [1990] discussed above. After impinging on the shelf break northeast of Taiwan, the Kuroshio turns northeastward and flows along the shelf break up to the area around 30.5°N, 129.0°E where it turns to eastward and then exits the ECS through the Tokara Strait. The strength and width of the modeled Kuroshio in the ECS are about 1 m s^{-1} and 100 km, respectively. Also evident is that the TWC originates from Taiwan Strait and flows strongly into the ECS. Initially, TWC flows northeastward as whole, and then divides into two branches near 27°N: one strong inshore branch and one weak offshore branch. The inshore branch flows northeastward near the 50 m isobath and finally into Tsushima Strait, while the offshore branch flows northeastward and joins into the mainstream of Kuroshio. However, it is worth noting that the KBCNT reported by *Kondo* [1985], cannot be found in the current distribution at the 20 m depth.

[21] In addition to the current distribution, the volume transports through four cross sections in Figure 5, are also compared with the results of previous researchers. The water on the continental shelf of ECS is mainly exchanged through the Taiwan Strait (TS), the Tsushima Strait (TUS), the Tokara Strait (TKS), and the section east of Taiwan (ET). The climatology run of Nest2 shows that the time-averaged volume transport through the TS is 1.03 Sverdrup (Sv), with a maximum (~2.32 Sv) in summer and a minimum (~0.18 Sv) in winter (Figure 6) which is consistent with the estimate (0.14 Sv) by *Teague et al.* [2003] on the basis of data from four moored ADCPs from October through December 1999. The time-averaged volume transport through sections ET (i.e., east of Taiwan) and TKS (i.e., Tokara Strait) are 21.37 and 20.66 Sv, respectively, while the seasonal variation of time-averaged volume transport through section ET as well as section TKS, is weak. The time-averaged volume transport

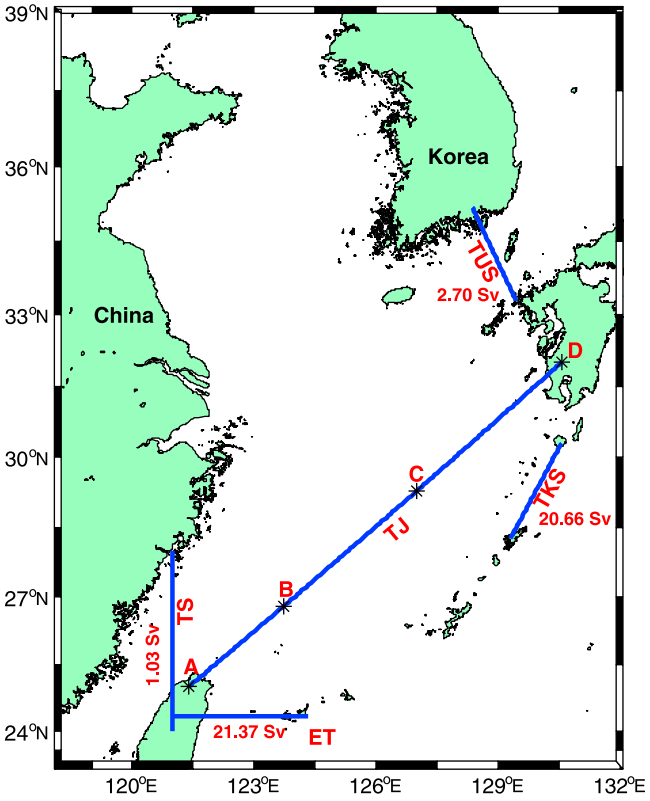

Figure 5. Cross sections where volume transports are calculated in Nest2.

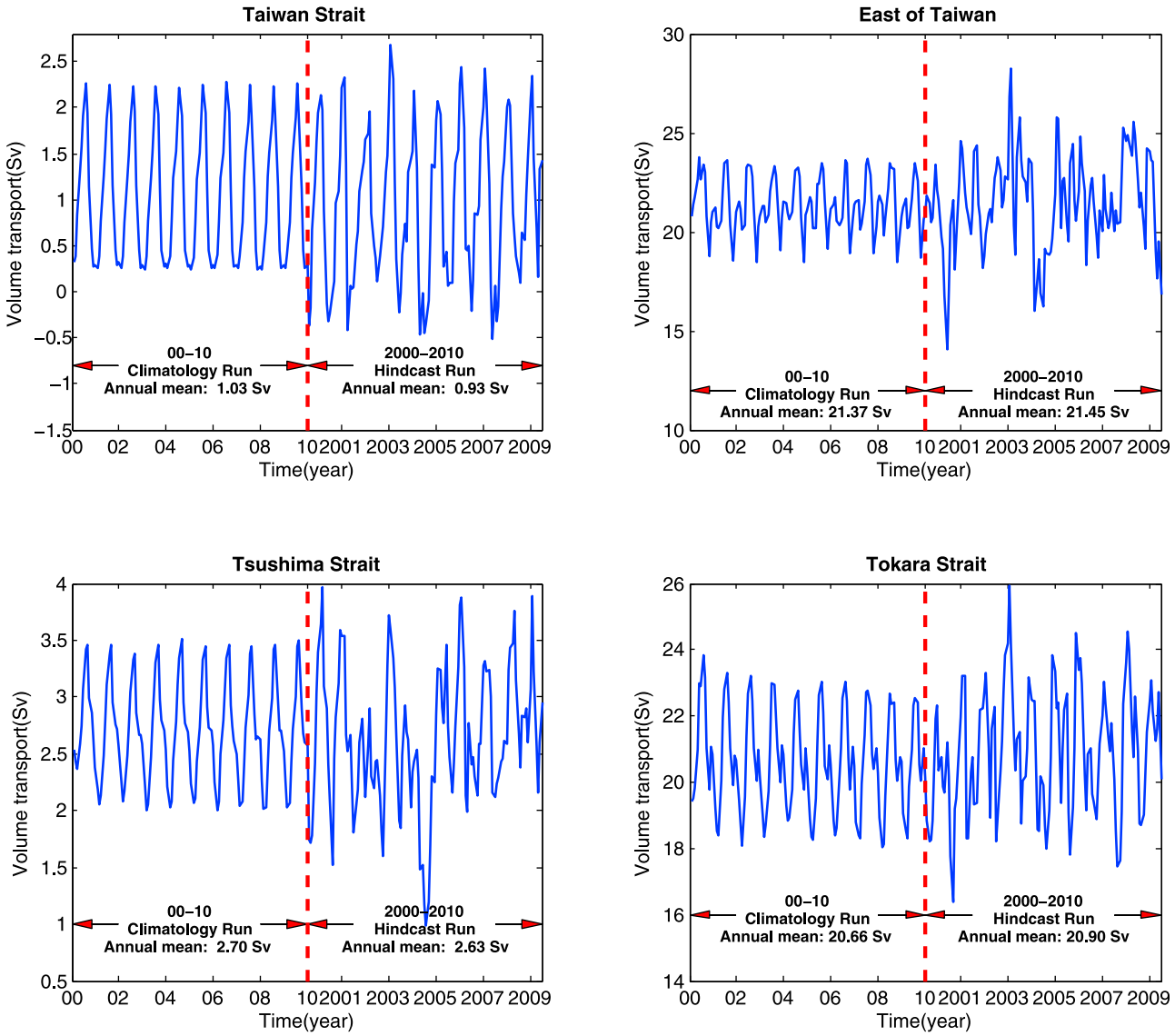

Figure 6. Time series of monthly mean volume transport through the entire water depth of four cross sections (see Figure 5).

through the section TUS (i.e., Tsushima Strait), is 2.70 Sv which is almost the same value as that (2.65 Sv) estimated by *Teague et al.* [2005] from observational data. It is worth noting that in the hindcast run (2000–2010) of Nest2, the volume transport of Taiwan Strait shows a clear interannual variation. In some years, the mean volume transport across the Taiwan Strait is negative (southward) in winter, thus supporting previous observations from *Jan et al.* [2006] that there is no persistent northward flowing current throughout the strait in winter. In addition, the hindcast run (2000–2010) of Nest2 also shows an annually mean volume transport 2.63 Sv across TUS which is surprisingly consistent with the averaged value 2.64 Sv over the 5.5 year observation period (21 February 1997 to 25 August 2002) [*Takikawa et al.* 2005]. For convenience to contrast with previous results, Table 1 is made to illustrate the differences among them. Interesting to note is that the volume transports of TUS and TS agree very well with the generally accepted value

Table 1. Annual Mean Water Fluxes Across Transects TUS, TS, ET, and TKS[a]

Source	East of Taiwan (Sv)	Tokara Strait (Sv)	Tsushima Strait (Sv)	Taiwan Strait (Sv)
Fang et al. [1991]				**2.10**
Feng et al. [2000]		**23.40**		
Teague et al. [2003]	23.00	**20.00**		
Wang et al. [2003]				**1.80**
Teague et al. [2005]			**2.65**	
Takikawa et al. [2005]			**2.64**	
Isobe [2008]			**2.65**	**1.20**
Lee and Chao [2003]	23.46		2.80	1.51
Guo et al. [2006]	23.83	19.47	3.03	1.72
Nest2 (climatology run)	21.37	20.66	2.70	1.03
Nest2 (hindcast run)	21.45	20.90	2.63	0.93

[a]Bold values are from observations; otherwise, data are from model results.

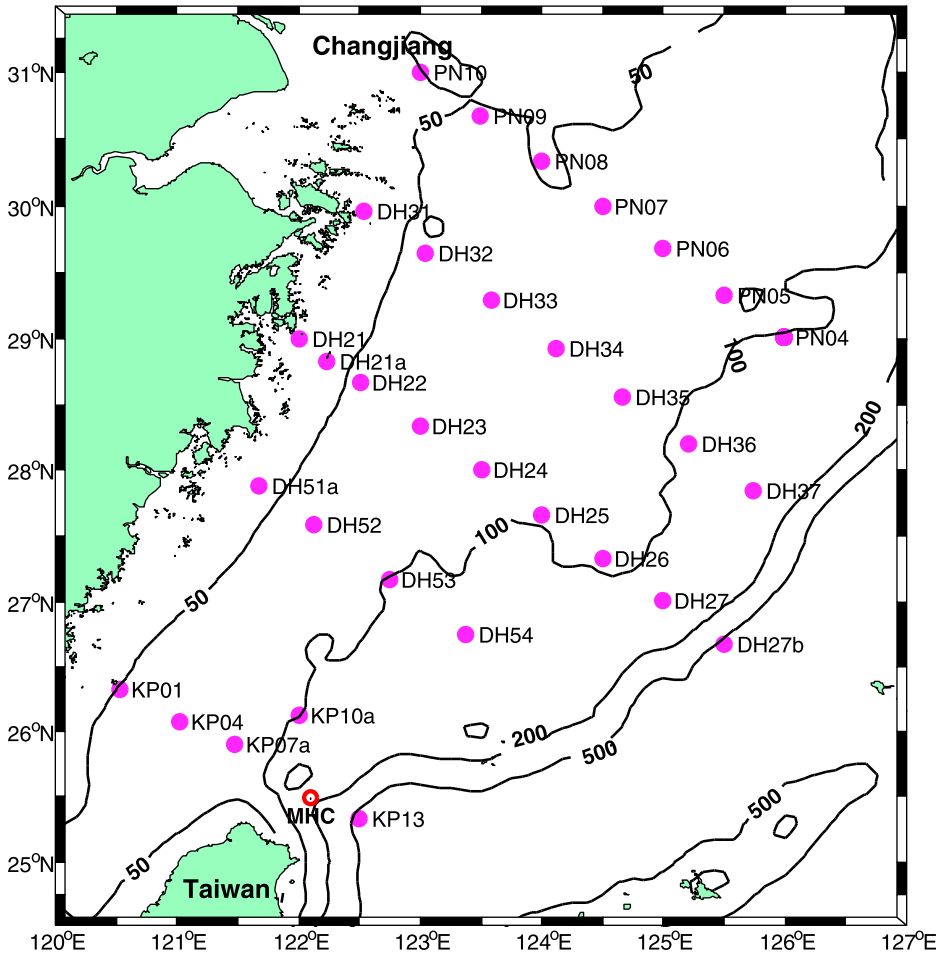

Figure 7. Sampling transects in August 2009. Transect KP comprises KP01, KP04, KP07a, KP10a, and KP13; transect DH5 comprises DH51–DH53; transect DH3 comprises DH31–DH37; and transect DH2 comprises DH21–DH27.

1.2 Sv in section TS and 2.65 Sv in section TUS [*Isobe*, 2008], respectively.

3.2. Vertical Salinity Distribution Comparison Between Observational Data and Model Results

[22] Thirty two stations were occupied by the ECS summer cruise conducted by the Xiamen University (XMU) in the period 15 August to 2 September 2009 along five transects normal to the coast of the ECS (Figure 7). The profiles of temperature and salinity were measured by conductivity-temperature-depth pressure sensors (CTD).

[23] To examine vertical structure of model results, hindcast results of Nest2 obtained during the same period as that of the actual cruise, were compared with the observed salinity distributions along transect of DH2, DH3, DH5 and KP. There are very good agreements between the observed and modeled salinity (Figures 8–11). The high-salinity cores in deep water (Figures 10 and 11), and less saline water in the central parts of the survey transects, are all clearly reproduced in the model results. The appropriate representation of the vertical structure of the salinity makes the Nest2 model strong enough to delineate the delicate structure of the KBBCNT.

[24] Salinity distributions in four cross transects (DH2, DH3, DH5, and KP; see Figures 8–11) demonstrate that in summer, high-salinity waters (S >34.2) exist in the deep water of the survey domain but not in the northern end part of the Taiwan Strait (see western stations KP01, KP04, and KP07a in Figure 8), and that in the central parts of the bottom waters of transects DH2 and DH3 (Figures 10 and 11), a less saline water (S <34.2) seems to separate saline core 1 from saline core 2 (Figures 10 and 11). The central low-salinity water is relatively homogeneous in contrast with the saline cores. From transect KP (Figure 8) and *Chung et al.* [2001, Figure 4], it can be found that in summer, the maximum salinity of the northern end part of Taiwan Strait is less than 34.2 which is worth bearing in mind. Therefore, the bottom high-salinity water, no doubt, does not originate from the Taiwan Strait Water (TSW), while the upper low-salinity water does stem mainly from the TSW. The TSW is the major water mass observed at the upper layers of transects, but does not account for all waters on them [*Su and Wong*, 1994]. At the same time, *Su et al.* [1994] pointed out that the surface water of TWC was formed by the mixing of Kuroshio surface water flowing northeastward with the Taiwan Strait Water, while the deep water originated from Kuroshio subsurface water east of Taiwan. *Guo et al.* [1985] guessed that there may be a channel through which the Kuroshio subsurface water flows onto the shelf of the ECS.

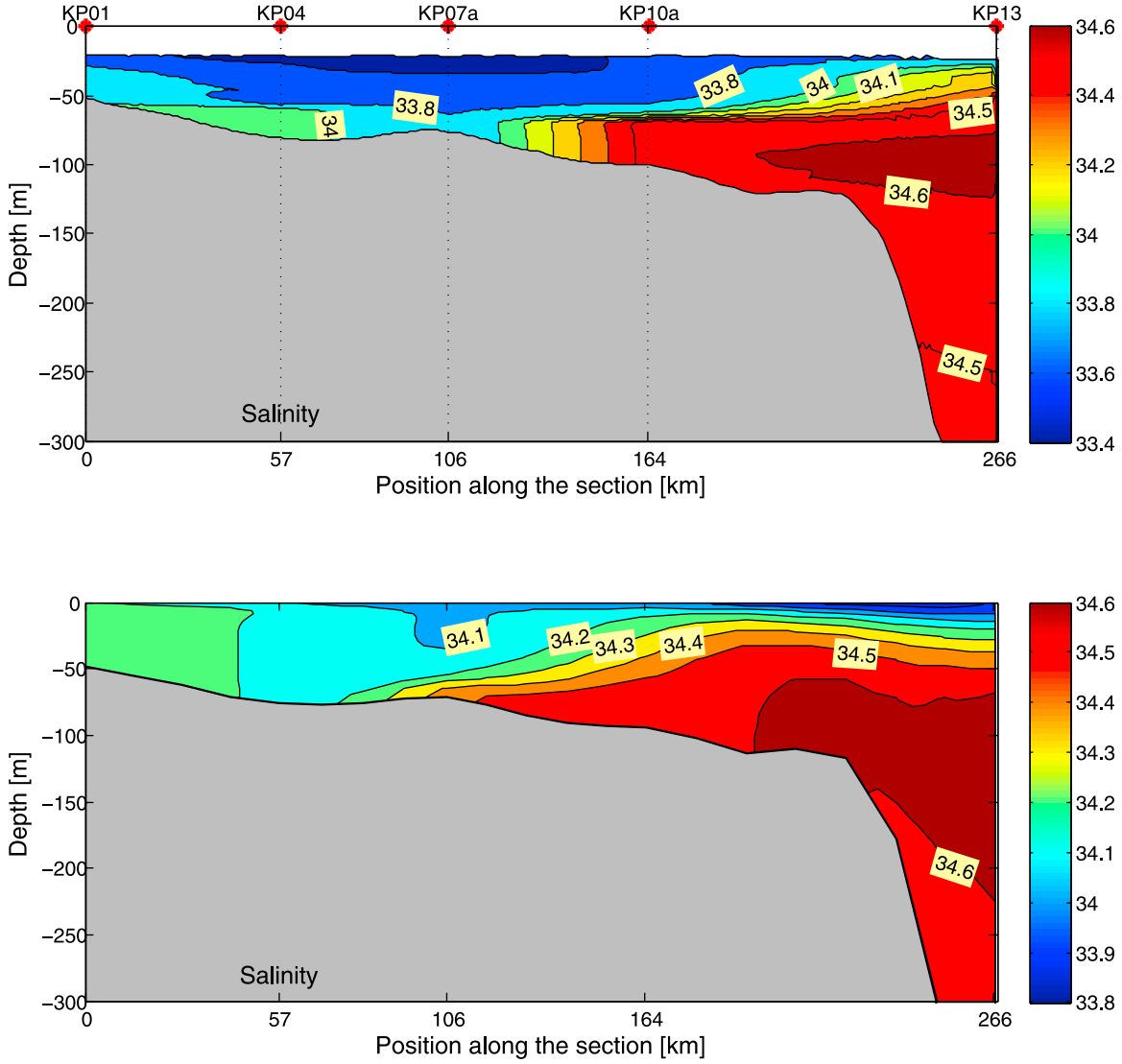

Figure 8. Cross sections of salinity for transect KP from (top) the summer cruise and (bottom) model results.

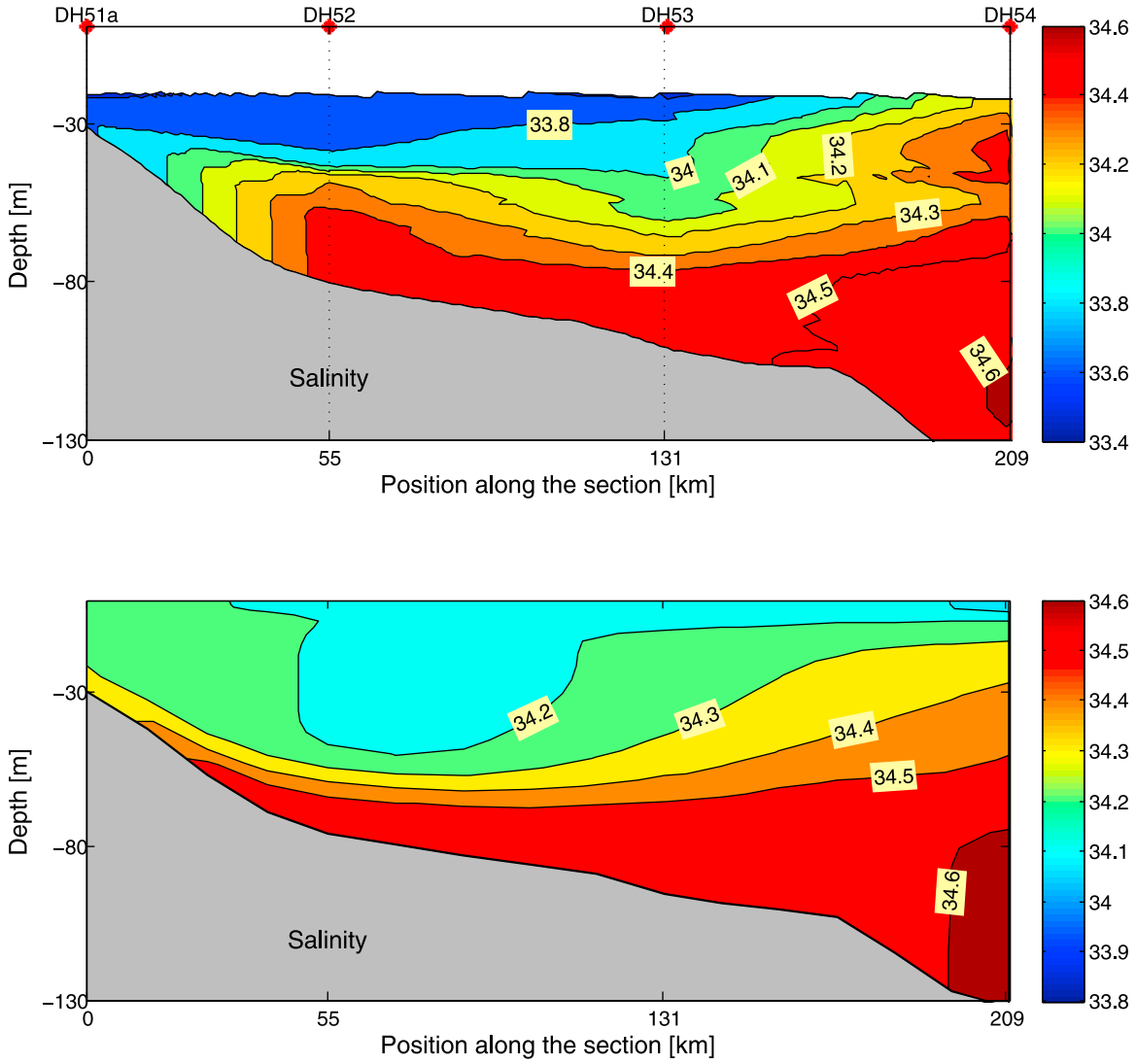

Figure 9. Same as Figure 8 except for transect DH5.

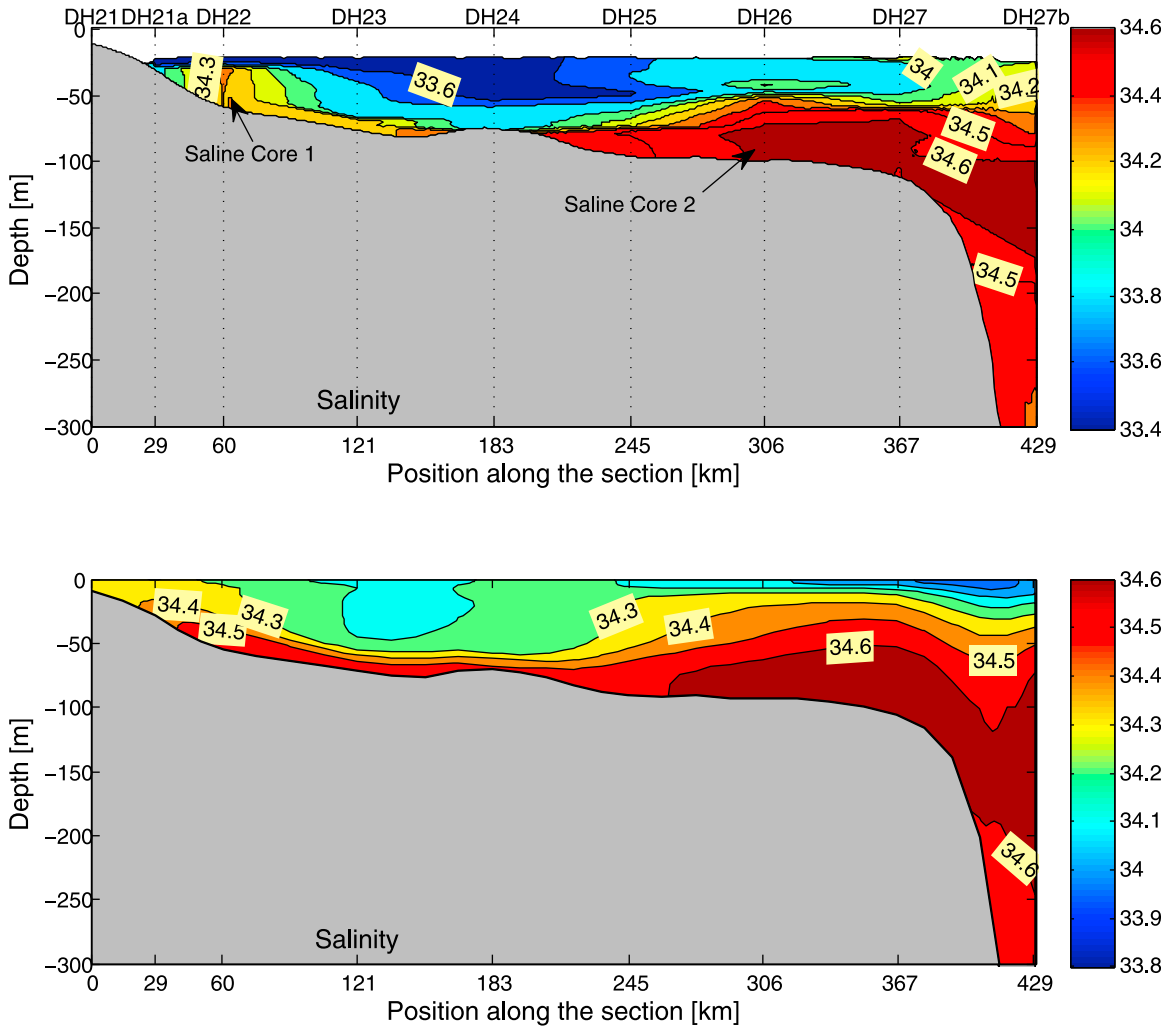

Figure 10. Same as Figure 8 except for transect DH2.

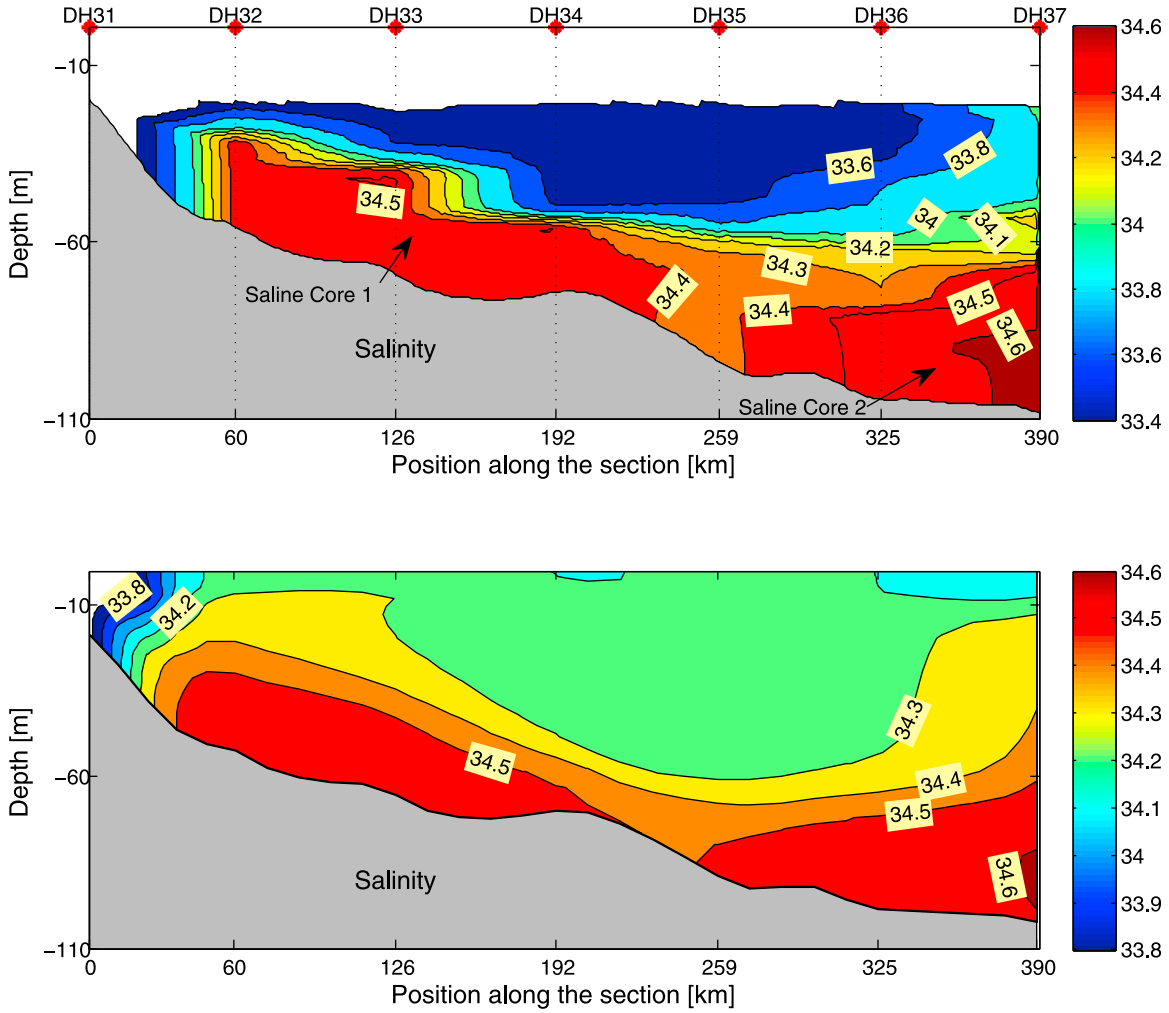

Figure 11. Same as Figure 8 except for transect DH3.

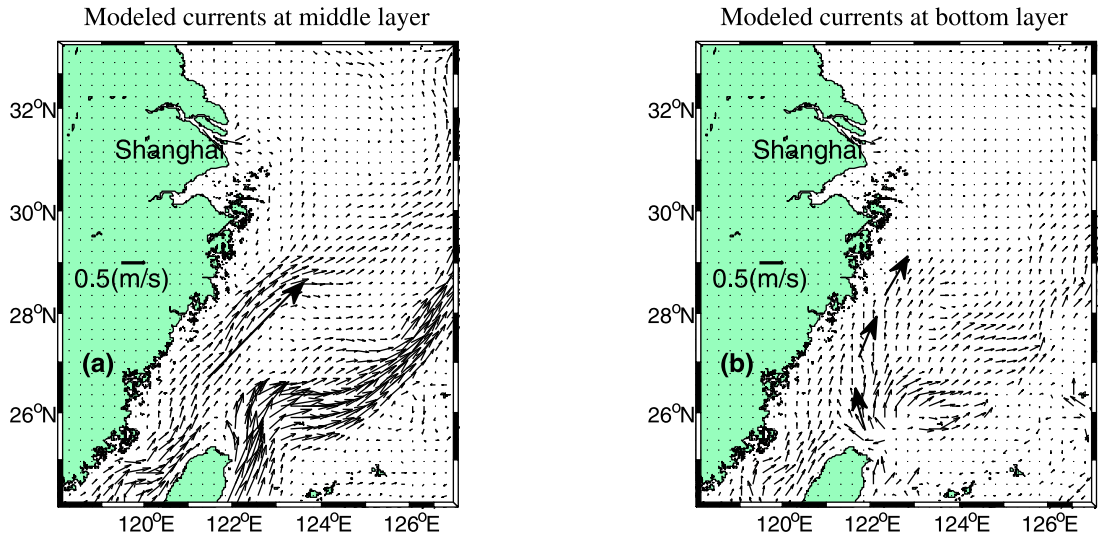

Figure 12. In *s* coordinates [*Song and Haidvogel*, 1994], monthly mean current distributions at (a) middle layer and (b) bottom layer in August 2009.

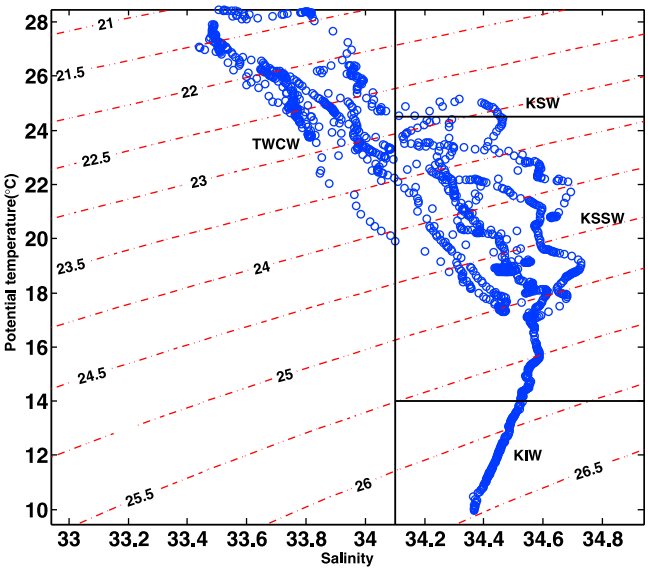

Figure 13. A plot of observed salinity and potential temperature below the depth of 20 m from 15 August to 2 September 2009 (see Figure 7). Taiwan Warm Current Water (TWCW), Kuroshio Surface Water (KSW), Kuroshio Subsurface Water (KSSW), and Kuroshio Intermediate Water (KIW) are marked, and dashed lines represent the potential density.

[25] In addition, the less saline water (S <34) derived from the Changjiang is not well reproduced in the model, because the time series (2000–2010) of observational salinity data of Changjiang River at the point sources of model domain are unavailable for us, and the salinity data of Changjiang River interpolated from COADS (its horizontal resolution is 1° × 1°; see *Diaz et al.* [2002]) has been used instead in the hindcast run.

3.3. Kuroshio Bottom Branch Current to the Northeast of Taiwan

[26] It is worth noting that the hindcast (August 2009) of Nest2 shows a Kuroshio Bottom Branch Current to the northeast of Taiwan (i.e., KBBCNT) in summer. Figure 12 shows that at the bottom layer (around 27.0°N, 121.5°E), the KBBCNT flows northwestward (big arrows in Figure 12b), different to the TWC (big arrow in Figure 12a) which flows northeastward at the middle layer. Salinity distributions in four cross transects (DH2, DH3, DH5, and KP; see Figures 8–11) confirms the circulation pattern of KBBCNT and TWC. By tracing the bottom cold water, *Su and Pan* [1987] pointed out that in the region around 26.0°N, 122.2°E, the bottom current is northward in spring and summer which also confirms the model results.

[27] Since the bottom pathway of Kuroshio subsurface water (i.e., the KBBCNT) is often subject to debate [*Kondo*, 1985; *Guan and Fang*, 2006; *Isobe*, 2008], the KBBCNT in summer is further discussed in section 4.

4. Discussion

4.1. Bottom Saline Water Observed in the Survey Domain in August 2009

[28] On the basis of the salinity and temperature data, water masses are classified according to the characteristic temperature and salinity of the water on the ECS shelf [*Liu et al.*, 2000; *Chen and Wang*, 2006; *Zhang et al.*, 2007]. A T-S diagram (Figure 13) is made only from the data beneath 20 m to focus on the characteristics of the deep and bottom water on the ECS shelf.

[29] Figures 14a and 14b show the horizontal distributions of salinity at 30 m depth and at deep and bottom layers, respectively. In the salinity distribution at the 30 m depth, it is immediately clear that the less saline water comes mainly from the Taiwan Strait according to the characteristic value of salinity 33.7 [*Su and Wong*, 1994], where the TWC flows northeastward in the central part of survey transects with saline waters on both sides. It is easy to understand that the eastern side saline water comes mainly from northward intruding subsurface Kuroshio water which flows northward, then turns anticyclonically and joins the western flank of the Kuroshio. However, north to the 28.5°N off the Zhejiang coast, there is also saline water on the west side of TWC. With respect to the origination of this saline water, *Hu et al.* [1984] pointed out that in summer, it was caused by the upwelling of deep water and elucidated further that the upwelling was not wind-driven, but controlled by a northward branch of Kuroshio. However, the bifurcation position of Kuroshio is not shown in his paper and also is the extension of the branch because of the scant data. For tracing the source of the west side saline water, the horizontal distributions of salinity at the deep and bottom layer are shown in Figure 14b, and it can be easily found that at the bottom layer, the west side saline water is linked continuously to the mainstream of Kuroshio. Interesting to note is that in Figure 14b, there is a saline tongue which originates from the subsurface water of Kuroshio to the northeast of Taiwan, extends northwestward gradually from 300 m to 60 m, then turns to northeast in the region around 27.5°N, 122°E, and finally reaches at 31°N off the mouth of the Changjiang River along about 60 m isobath. And besides this, in the central parts of northern transects (Figure 14b), there is a less saline water (<34.1) which seems to separate the saline tongue from the eastern saline water which is the upwelled subsurface Kuroshio waters near the shelf break of the ECS [*Su and Wong*, 1994; *Liu et al.*, 2000]. Explicitly, the saline tongue (Figure 14b) is a strong indicator that there is a northwestward flowing current (i.e., KBBCNT).

[30] Regarding the source of saline core 1 (Figures 10 and 11), it, explicitly, is very unlikely that the bottom waters at stations DH32–33 and DH22 could have come from the east across the shelf of the ECS since the bottom Ekman pumping [*Pedlosky*, 1979] are not strong enough for waters deeper than 200 m to climb shoreward to the 60 m isobath. Therefore it is very likely that there is a Kuroshio branch denoted by dash line arrows in Figure 14b, which is bifurcated from the subsurface water of Kuroshio off northeastern Taiwan, and intrudes northwestward onto the shelf, carrying high-salinity water. In detail, Figures 9, 10, and 11 show that at transect DH5, it is difficult to distinguish the branch of Kuroshio from the mainstream of Kuroshio, but the more northern the transect is, the easier it is to be identified.

[31] In light of above analysis of the salinity characteristics, it is proposed that the bottom saline tongue is formed by a Kuroshio Bottom Branch Current to the northeast of Taiwan (i.e., KBBCNT).

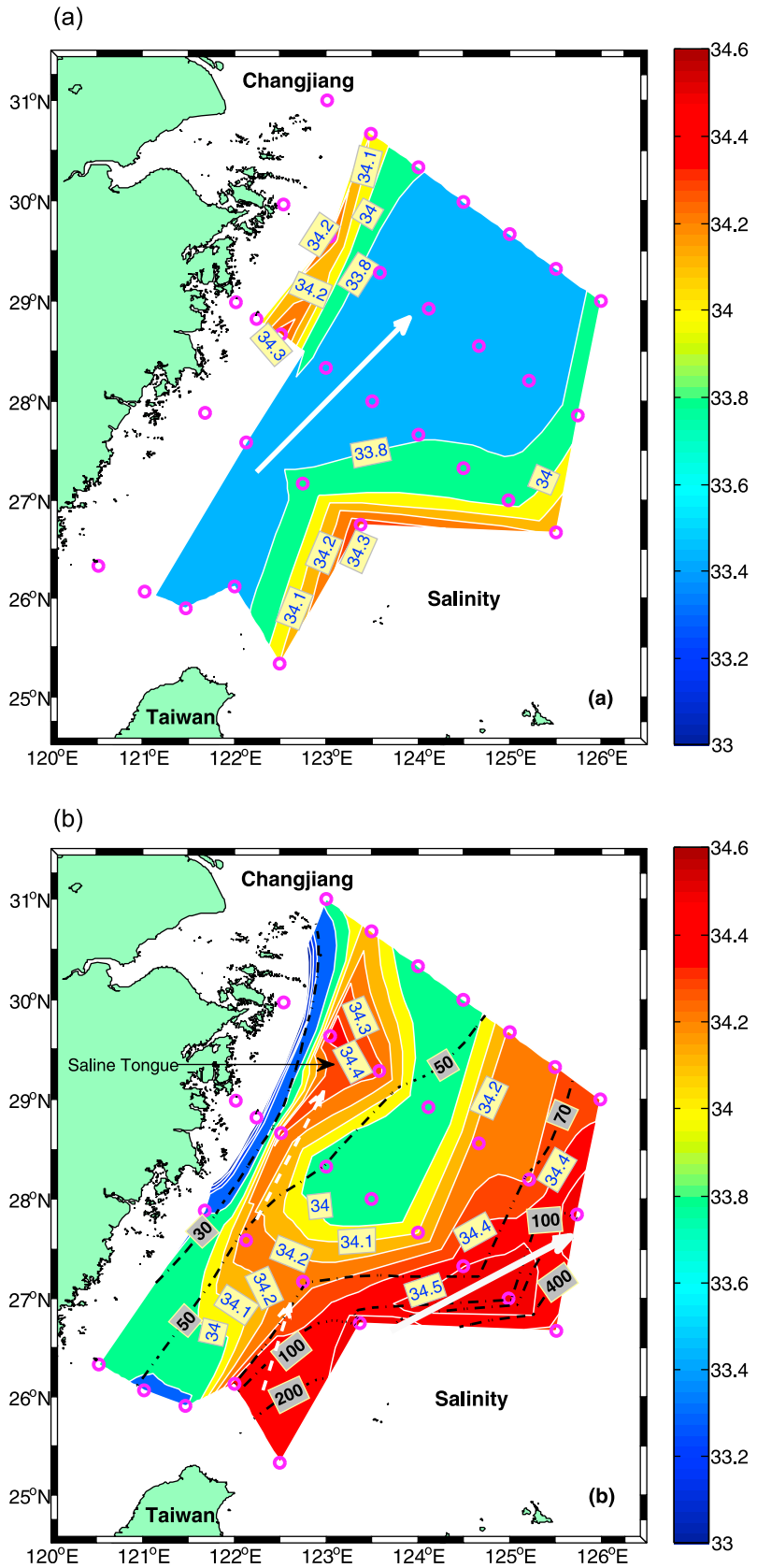

Figure 14. Distributions of salinity at (a) 30 m depth and (b) deep and bottom layers on which the depths (dash-dotted lines) of the data are overlapped. Circles indicate the hydrographic stations, and the dashed arrows indicate the possible current. The thick, solid arrows indicate Taiwan Warm Current in Figure 14a and Kuroshio in Figure 14b, respectively.

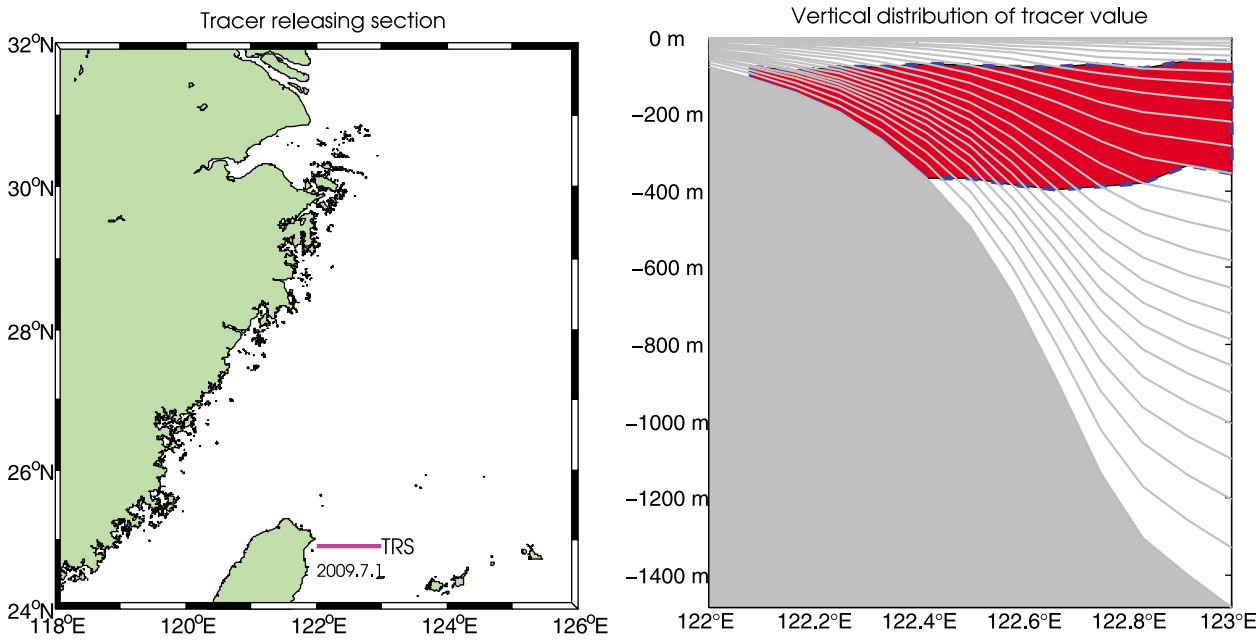

Figure 15. (left) Tracer-releasing section (TRS) and (right) vertical distributions of tracer value in tracer experiments 1 and 2.

[32] Being lack of direct current measurements, numerical model (Nest2) is used to investigate the formation of the saline tongue off the coast of Zhejiang (Figure 1), and to clarify the pathway of the KBBCNT in detail. Passive tracer experiments are adopted to represent its horizontal and vertical distributions on the shelf of ECS, and particles experiment to elucidate the track of the water of KBBCNT.

4.2. Passive Tracer Experiments

[33] Tracer experiments 1 and 2 were carried out to elucidate the features of the KBBCNT. In tracer experiment 1, the distribution of tracer is controlled by the advection and diffusion terms, while in tracer experiment 2, the tracer is transported only by the advection term. In both tracer experiments, the tracer is released along a section TRS in Figure 15 on 1 July 2009, and then the tracer value is fixed to 100 after that time. The formulations of both tracer experiments are offered as follows.

4.2.1. Tracer Experiment 1

[34]

$$\frac{\partial C}{\partial t} + \vec{V} \bullet \nabla C = -\frac{\partial}{\partial z}\left(\overline{C'W'} - \nu_\theta \frac{\partial C}{\partial z}\right) + F_C + D_C$$

$$F_C = \begin{cases} 100.0 & \text{filled area in the right panel of Figure 15} \\ 0.0 & \text{elsewhere} \end{cases}$$

4.2.2. Tracer Experiment 2

[35]

$$\frac{\partial C}{\partial t} + \vec{V} \bullet \nabla C = F_C$$

$$F_C = \begin{cases} 100.0 & \text{filled area in the right panel of Figure 15} \\ 0.0 & \text{elsewhere} \end{cases}$$

where the variables are defined as follows: C, passive tracer; D_C, horizontal diffusive terms; F_C, forcing term; ν_θ, molecular diffusivity; $\overline{C'W'}$, turbulent tracer flux which is parameterized as $\overline{C'W'} = -K_C \frac{\partial C}{\partial z}$. An over bar represents a time average and a prime represents a fluctuation about the mean.

[36] Figure 16 shows the distributions of tracer value from tracer experiment 1 and 2 along transect DH3. To our surprise, each saline core of DH3 is represented by a high trace value core. It means that the saline water at the bottom layer of transect DH3 comes from subsurface water of Kuroshio at section TRS. The mixing process may affect the distribution feature of the tracer value to the extent that the distribution of tracer value does not represent the really distribution of the Kuroshio subsurface water. To clarify the question, tracer experiment 2 was carried out. Figure 16 demonstrates that the high tracer core distribution is mainly controlled by advection process, though the mixing process is important. Therefore, the saline water of saline core 1 in DH3, no doubt, stems from the Kuroshio subsurface water east of Taiwan.

[37] The tracer distributions at middle layer and bottom layer are represented by Figure 17 to depict the horizontal distribution of the Kuroshio subsurface water. It is satisfactory that the salinity distribution features (Figures 14a and 14b) are reproduced again by the tracer value distribution in Figure 17. The low-salinity area in Figure 14a is occupied by the low tracer value area in Figure 17 (left); and on the both sides of low-salinity area of Figure 14a, there are two high-salinity areas which are also reproduced by the distribution of high tracer value in Figure 17 (left). In the tracer distribution at the bottom layer, the same situation appears again that the tracer value exactly delineate the feature of the saline tongue in Figure 14b. Thus, tracer experiments tell us that the bottom saline waters might very well originate from the Kuroshio subsurface water east of Taiwan (filled area of Figure 15, right). For these reasons, it is most reasonable that the trajectories of tracers from the Nest2 model will be believable.

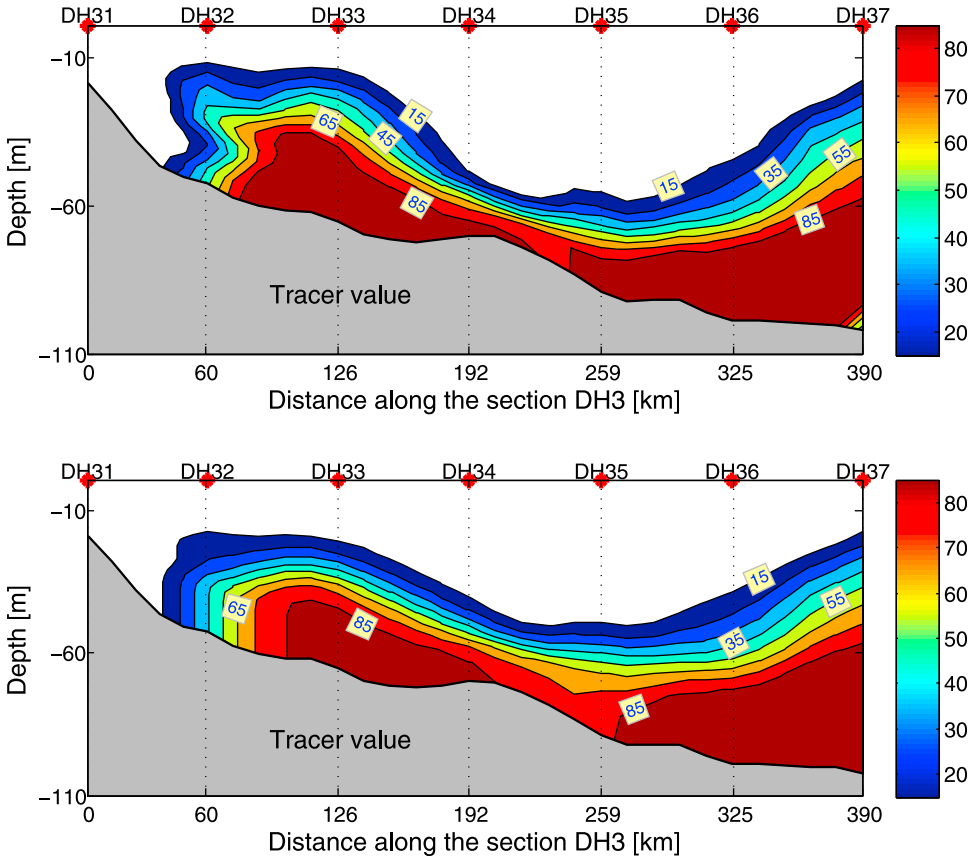

Figure 16. The vertical distribution of the 5 day (28 August to 1 September 2009) running mean of tracer value from (top) tracer experiment 2 and (bottom) tracer experiment 1. Contour interval is 15.

[38] In a word, if the tracer is released along section TRS (Figure 15), we can gain most of the features of the salinity distribution on the shelf of the ECS. To see clearly the trajectories of tracers, a particle tracking experiment was done.

4.3. Particle Tracking Experiment

[39] The hindcast duration of Nest2 is from 1 January 2000 to 1 January 2010, while the particles are released on 1 July 2009 in Nest2 model to simulate the feature of KBBCNT in the duration of summer cruise. Figure 18 demonstrates the initial locations of particles and the trajectories of the particles.

[40] Obviously, these trajectories can be classified into two typical current patterns: Kuroshio mainstream (trajectories of particles 2 and 3), and KBBCNT (trajectory of particle 1). Particles 2 and 3 are released near 240 m depth, and the

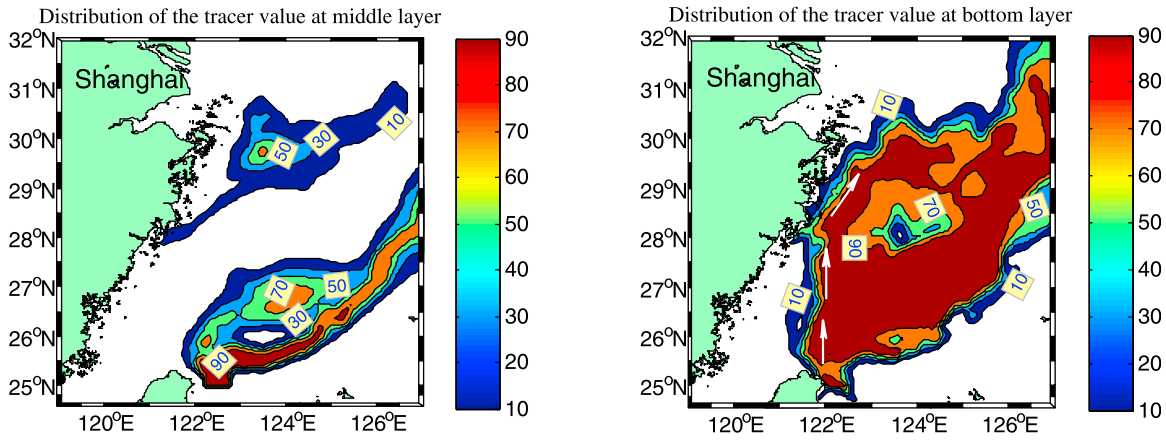

Figure 17. In *s* coordinates [*Song and Haidvogel*, 1994], distributions of the 5 day (28 August to 1 September 2009) running mean of tracer value at the (left) middle layer and (right) bottom layer. Contour interval is 10. Arrows indicate the possible KBBCNT.

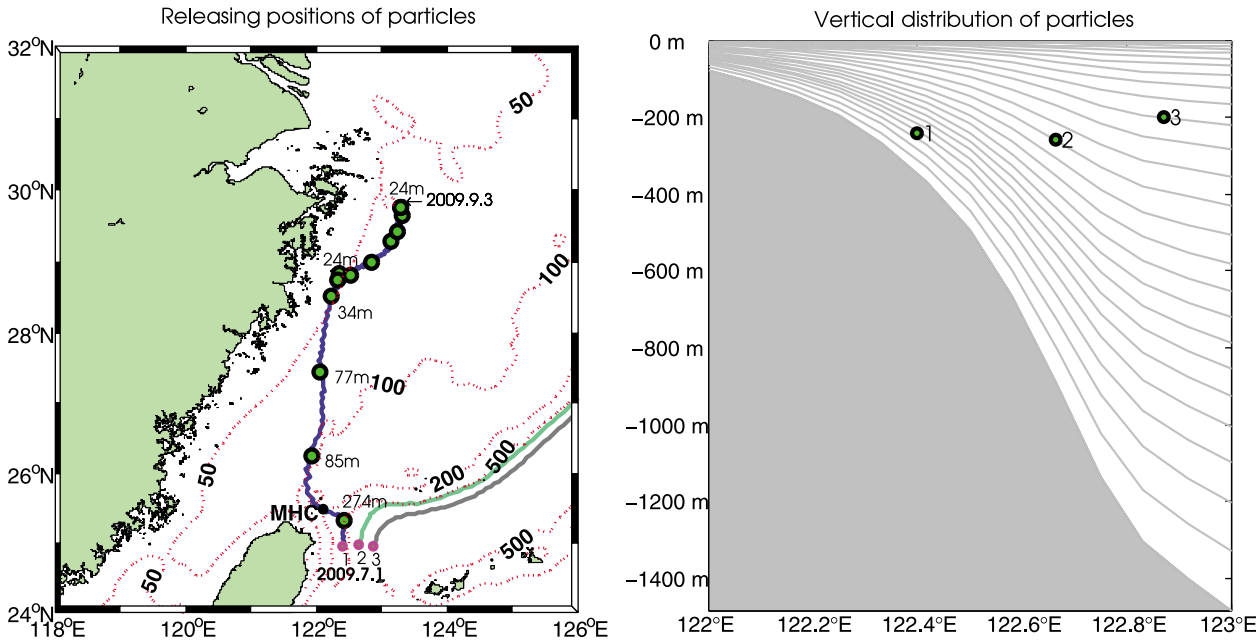

Figure 18. Releasing locations of (left) particles and (right) their vertical distributions. Circles are marked every 4.5 days together with the depths of particles. The points and numbers (1, 2, and 3) indicate the initial locations of particles. Dashed lines denote the isobaths of 50, 100, 200, and 500 m.

trajectories of them clearly delineate the track of the mainstream of Kuroshio which flows along the shelf break of the ECS. The most noteworthy feature of the tracks is that released near 240 m, particle 1 supplies us with a surprising trajectory which originates from the subsurface water of Kuroshio, then runs northwestward through the channel between MHC and Taiwan, next upwells northward gradually from 158 to 71 m, is trapped by the upwelling off the coast of Zhejiang province at 29°N staying there for 20 days, and finally reaches at 30°N trapped by upwelling there again. This trajectory is exactly coincident with the location of saline tongue of Figure 14b. According to the trajectory of particle 1, it is no doubt that the KBBCNT does exist and the saline water carried by it causes saline core 1 off the coast of Zhejiang.

[41] On the basis of the above analysis, we propose that there is a current (i.e., KBBCNT) which originates from Kuroshio subsurface water, upwells northwestward gradually from 300 to 60 m northeast of Taiwan, then turns to northeast in the region around 27.5°N, 122°E, and finally reaches at 31°N off the mouth of the Changjiang River following about 60 m isobaths, carrying high-salinity water. The TWC flows, like an overpass, northeastward over the KBBCNT (Figure 19). The pathway of the KBBCNT is different to the KBCNT [see *Ichikawa and Beardsley*, 2002, Figures 6 and 10]. The KBCNT cannot explain simultaneously the central low-salinity water and saline core 1 in DH3 (Figure 11). This question can be avoided by the pathway of KBBCNT which causes saline core 1 in DH3 and the central low-salinity water in DH3 is caused by TWC which strides over the KBBCNT (Figure 19).

[42] The ADCP observations conducted by various researchers demonstrate that the connectivity of the volume transport is incomplete between the Tsushima (2.6 Sv) and Taiwan Straits (1.2 Sv) [*Isobe*, 2008]. The remaining 1.4 Sv must be supplied by the onshore Kuroshio intrusion crossing the East China Sea shelf break. The KBBCNT, no doubt, have played a very important role in this process. Figure 20 shows the volume transport distribution along the section between Taiwan and Japan (TJ in Figure 5) in summer. The Kuroshio intrusion occurs in several places along section TJ, most notably to the northeast of Taiwan and to the southwest of Kyushu. In summer, the volume transport of the KBBCNT and KBC together is about 1.64 Sv in Figure 20. Therefore, a lot of materials can be transported from the east of Taiwan to the area off the mouth of the Changjiang River by the KBBCNT.

[43] As regards the dynamic mechanism of the KBBCNT, as *Su et al.* [1994] pointed out, in the western boundary current, the cross-stream momentum equation is approximately geostrophic. Therefore, in the eastern side of Kuroshio, the height of the free surface is higher than that in the western side in summer. It is also true that in the eastern part of Taiwan Strait, the height of the free surface is higher than that of western part. Therefore, it is easily to understand that Kuroshio has a tendency to turn to left, when the Kuroshio flows northward enough to loss the blocking of Taiwan Island. In a similar way, the TWC will turn to east after it flow out of the Taiwan Strait, being lack of the blocking of Taiwan Island on its eastern side. Thus there will be a collision between the TWC and the KBC (Figure 1) in the surface water near 26°N where the KBC turns to northeast and has a tendency to join the mainstream of Kuroshio. The offshore branch of TWC may be created from the collision. In fact, in upper layer the Kuroshio is so strong that it prevent the TWC from turning to east and limits the TWC to the 50 m isobath after Kuroshio flows northward past Taiwan Island. And besides this, north of Taiwan the shelf break turns

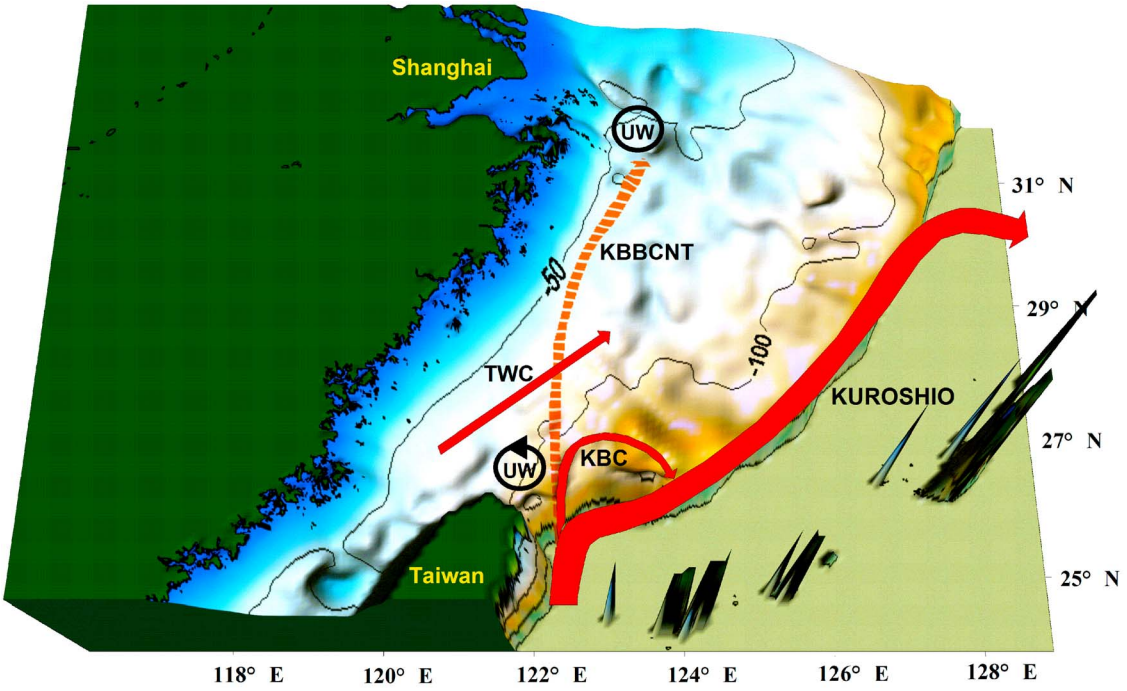

Figure 19. Summer ocean circulation pattern schematically represented in a three-dimensional shaded relief, rendering from bathymetry of the East China Sea where depth >500 m is equal to 500 m for simplification. Solid thin lines represent the isobaths of 50, 100, 200, and 500 m. The dashed red line represents the possible ocean currents (KBBCNT), and UW denotes upwelling.

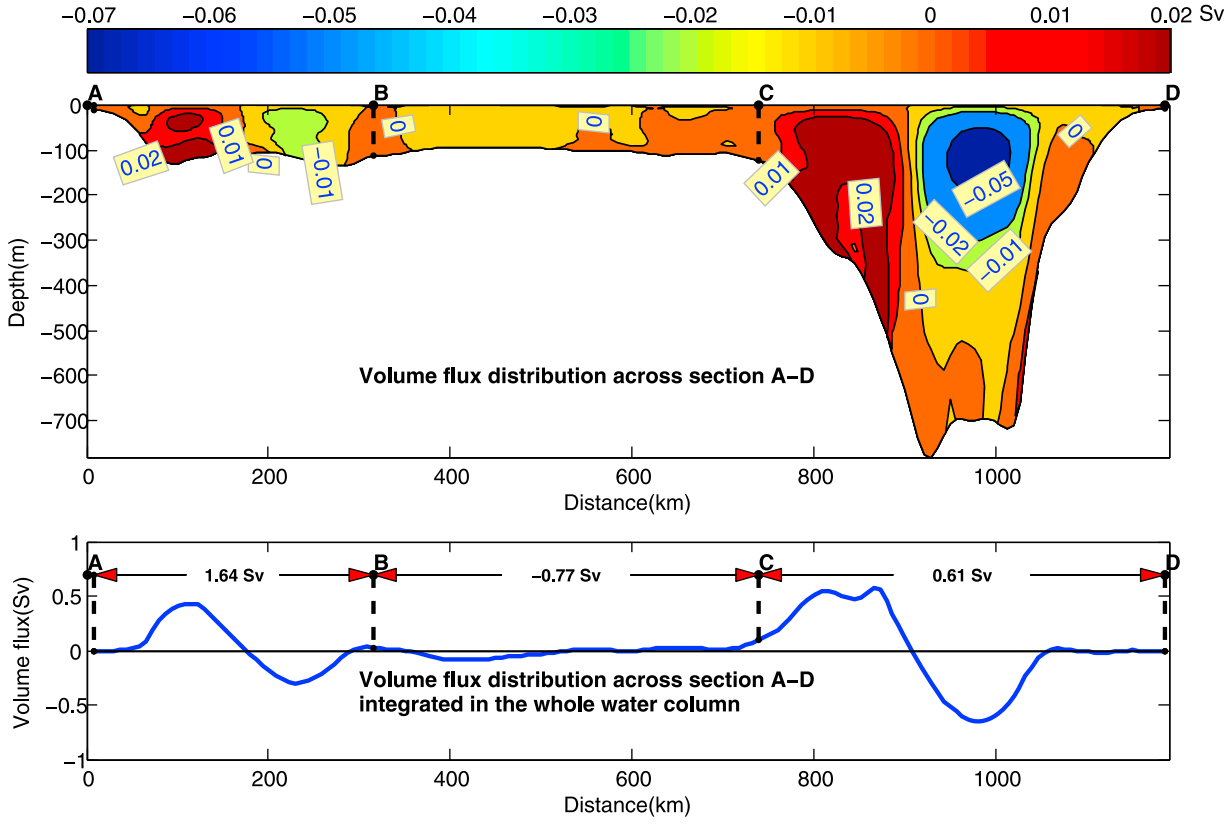

Figure 20. Monthly mean volume transports across the section TJ in August (see Figure 5), where the negative volume transport denotes an offshore flux, and positive volume transport denotes an onshore flux. Contour interval is 0.01 Sv.

sharply to the east, which traps the Kuroshio and makes it to flow northeastward along the shelf break. So, off the northern coast of Taiwan, there will be a pressure gradient which points to the north. In view of the lighter TWCW, the intrusion of Kuroshio in the upper layer cannot benefit from the pressure gradient. Nevertheless, in the deeper water, the dense subsurface water of Kuroshio is favorable to impinge onto the shelf, driven by the pressure gradient and inertial effect of Kuroshio. In addition, between MHC (Figure 1.) and Taiwan Island, there is a channel (Figure 19) which allows the subsurface water of Kuroshio to impinge onto the continental shelf of the ECS. This channel is exactly the place which the KBBCNT derives from; and the strength of KBBCNT depends on the width and the depth of this channel.

5. Conclusion

[44] The high-resolution model (Nest2) is accurate enough to reproduce volume transport (1.03 Sv) through the Taiwan Strait and volume transport (2.70 Sv) through the Tsushima Strait which is closer to recent observation value than former model results. At the same time, the model results have reproduced almost all of the known circulation structure on the ECS continental shelf. In addition, the hindcast of 2009 has reproduced the bottom high-salinity distribution characteristics of the salinity data from the summer cruise from 15 August to 2 September 2009.

[45] Tracer experiments show that the bottom high-salinity distribution on the shelf of ECS is caused by the intrusion of the KBBCNT, which has transported the saline Kuroshio subsurface water east of Taiwan to the area off the coast of Zhejiang. Furthermore, particles experiment gives the pathway of KBBCNT.

[46] On the basis of field observation data and model results, it is proposed that there is a current (i.e., KBBCNT) which originates from Kuroshio subsurface water, upwells northwestward gradually from 300 to 60 m northeast of Taiwan, then turns to northeast in the region around 27.5°N, 122°E, and finally reaches at 31°N off the mouth of the Changjiang River along about 60 m isobaths, carrying the high-salinity subsurface water of Kuroshio. The pathway of the KBBCNT is different to the KBCNT. The new circulation pattern of TWC and KBBCNT (Figure 19) can explain simultaneously the central low-salinity water and saline core 1 in DH3 (Figure 11), but the KBCNT [*Ichikawa and Beardsley*, 2002, Figures 6 and 10] cannot. The current pattern shown in Figure 19 roughly agrees with the TWC [*Guan*, 1978] in the upper layer and with the KBCNT [*Kondo*, 1985] in the deep and bottom layer. In addition, the volume transport of KBBCNT and KBC together, is also estimated to 1.64 Sv in summer. As *Zhang et al.* [2007] pointed out, the Kuroshio subsurface water is rich in phosphate. Therefore, in summer the KBBCNT can transport continuously the phosphate from the east of Taiwan to the area off the mouth of the Changjiang River where harmful algal bloom occurs frequently in summer.

[47] **Acknowledgments.** This paper was supported by the 973 Project (2009CB421205), the National Natural Science Foundation of China through grants 40806009 and 40976008, the Innovation Project of Chinese Academy of Sciences (KZCX2-EW-209), the Innovation Group Project of Chinese Academy of Sciences (KZCX2-YW-Q07-01 and KZCX2-YW-208-03), and the 908 Project (908-01-BC12).

References

Chang, P.-H., and A. Isobe (2003), A numerical study on the Changjiang diluted water in the Yellow and East China Seas, *J. Geophys. Res.*, *108*(C9), 3299, doi:10.1029/2002JC001749.

Chen, C.-T. A., and S. L. Wang (2006), A salinity front in the southern East China Sea separating the Chinese coastal and Taiwan Strait waters from Kuroshio waters, *Cont. Shelf Res.*, *26*, 1636–1653, doi:10.1016/j.csr.2006.05.003.

Chern, C. S., and J. Wang (1989), On the water masses at northern offshore area of Taiwan, *Acta Oceanogr. Taiwan.*, *22*, 14–32.

Chern, C. S., and J. Wang (1990), On the Kuroshio Branch Current north of Taiwan, *Acta Oceanogr. Taiwan.*, *25*, 55–64.

Chung, S. W., S. Jan, and K. K. Liu (2001), Nutrient fluxes through the Taiwan Strait in spring and summer in 1999, *J. Oceanogr.*, *57*, 47–53, doi:10.1023/A:1011122703552.

Diaz, H., C. Folland, T. Manabe, D. Parker, R. Reynolds, and S. Woodruff (2002), Workshop on advances in the use of historical marine climate data, *World Meteorol. Org. Bull.*, *51*, 377–380.

Egbert, G. D., and S. Y. Erofeeva (2002), Efficient inverse modeling of barotropic ocean tides, *J. Atmos. Oceanic Technol.*, *19*, 183–204, doi:10.1175/1520-0426(2002)019<0183:EIMOBO>2.0.CO;2.

Fang, G., B. Zhao, and Y. Zhu (1991), Water volume transport through the Taiwan Strait and the continental shelf of the East China Sea measured with current meters, in *Oceanography of Asian Marginal Seas*, edited by K. Takano, pp. 345–358, doi:10.1016/S0422-9894(08)70107-7, Elsevier, New York.

Feng, M., H. Mitsutera, and Y. Yoshikawa (2000), Structure and variability of the Kuroshio Current in Tokara Strait, *J. Phys. Oceanogr.*, *30*, 2257–2276, doi:10.1175/1520-0485(2000)030<2257:SAVOTK>2.0.CO;2.

Guan, B. X. (1978), A sketch of the current system of the East China Sea, in *Collected Papers of the Continental Shelf of the East China Sea* (in Chinese), pp. 126–133, Inst. of Oceanol., Chin. Acad. of Sci., Qingdao, China.

Guan, B. X. (1994), Patterns and structures of the currents in Bohai, Huanghai and East China Seas, in *Oceanology of China Seas*, vol. 1, edited by D. Zhou et al., pp. 17–26, Kluwer Acad., Dordrecht, Netherlands.

Guan, B. X. (2002), *Winter Counter-Wind Current off the Southeastern China Coast* (in Chinese), Ocean Univ. of China Press, Qingdao.

Guan, B. X., and G. Fang (2006), Winter counter-wind currents off the southeastern China coast: A review, *J. Oceanogr.*, *62*, 1–24, doi:10.1007/s10872-006-0028-8.

Guan, B. X., and H. L. Mao (1982), A note on circulation of the East China Sea, *Chin. J. Oceanol. Limnol.*, *1*, 5–16, doi:10.1007/BF02852887.

Guo, B. H., K. Lin, and W. X. Song (1985), The problems on flowing of the sea water in the southern East China Sea in summer (in Chinese with English abstract), *Acta Oceanol. Sin.*, *7*, 143–153.

Guo, B. H., Z. Z. Huang, and P. Y. Li (2004), *Ocean Environment of China Coast Sea and Adjacent Sea Areas* (in Chinese), China Ocean Press, Beijing.

Guo, X. Y., H. Hukuda, Y. Miyazawa, and T. Yamagata (2003), A triply nested ocean model for simulating the Kuroshio—Roles of horizontal resolution on JEBAR, *J. Phys. Oceanogr.*, *33*, 146–169, doi:10.1175/1520-0485(2003)033<0146:ATNOMF>2.0.CO;2.

Guo, X. Y., Y. Miyazawa, and T. Yamagata (2006), The Kuroshio onshore intrusion along the shelf break of the East China Sea: The origin of the Tsushima Warm Current, *J. Phys. Oceanogr.*, *36*, 2205–2231, doi:10.1175/JPO2976.1.

Hasumi, H., H. Tatebe, T. Kawasaki, M. Kurogi, and T. Sakamoto (2010), Progress of North Pacific modeling over the past decade, *Deep Sea Res. Part II*, *57*, 1188–1200, doi:10.1016/j.dsr2.2009.12.008.

Hishida, M. (1994), On the variation of oceanographic conditions in the source area of the Tsushima Warm Current, in *Proceedings of China-Japan JSCRK*, pp. 212–225, China Ocean Press, Beijing.

Hu, D. X., L. H. Lu, Q. C. Xiong, Z. X. Ding, and S. C. Sun (1984), On the cause and dynamical structure of the coastal upwelling off Zhejiang province, *Stud. Mar. Sin.*, *21*, 101–112.

Ichikawa, H., and R. C. Beardsley (2002), The current system in the Yellow and East China seas, *J. Oceanogr.*, *58*, 77–92, doi:10.1023/A:1015876701363.

Isobe, A. (2008), Recent advances in ocean-circulation research on the Yellow Sea and East China Sea shelves, *J. Oceanogr.*, *64*, 569–584, doi:10.1007/s10872-008-0048-7.

Jan, S., D. D. Sheu, and H.-M. Kuo (2006), Water mass and throughflow transport variability in the Taiwan Strait, *J. Geophys. Res.*, *111*, C12012, doi:10.1029/2006JC003656.

Kako, S., A. Isobe, S. Yoshioka, P.-H. Chang, T. Matsuno, S.-H. Kim, and J.-S. Lee (2010), Technical issues in modeling surface-drifter behavior on the East China Sea shelf, *J. Oceanogr.*, *66*, 161–174, doi:10.1007/s10872-010-0014-z.

Kondo, M. (1985), Oceanographic investigations of fishing grounds in the East China Sea and Yellow Sea—Part I. Characteristics of the mean temperature and salinity distributions measured at 50 m and near the bottom (in Japanese with English abstract), *Bull. Seikai Reg. Fish. Lab.*, *62*, 19–55.

Large, W. G., J. C. McWilliams, and S. C. Doney (1994), Oceanic vertical mixing: A review and a model with a nonlocal boundary layer parameterization, *Rev. Geophys.*, *32*, 363–403, doi:10.1029/94RG01872.

Lee, H. J., and S. Y. Chao (2003), A climatological description of circulation in and around the East China Sea, *Deep Sea Res. Part II*, *50*, 1065–1084, doi:10.1016/S0967-0645(03)00010-9.

Lee, J.-S., and T. Matsuno (2007), Intrusion of Kuroshio Water onto the continental shelf of the East China Sea, *J. Oceanogr.*, *63*, 309–325, doi:10.1007/s10872-007-0030-9.

Liang, X. S., and J. L. Su (1994), A two-layer model for the circulation of the East China Sea (in Chinese with English abstract), *Donghai Mar. Sci.*, *12*, 1–20.

Liang, W. D., T. Y. Tang, Y. J. Yang, M. T. Ko, and W. S. Chuang (2003), Upper-ocean currents around Taiwan, *Deep Sea Res. Part II*, *50*, 1085–1105, doi:10.1016/S0967-0645(03)00011-0.

Liu, K. K., T. Y. Tang, G. C. Gong, L. Y. Chen, and F. K. Shiah (2000), Cross-shelf and along-shelf nutrient fluxes derived from flow fields and chemical hydrography observed in the southern East China Sea off northern Taiwan, *Cont. Shelf Res.*, *20*, 493–523, doi:10.1016/S0278-4343(99)00083-7.

Marchesiello, O., J. C. McWilliams, and A. Shchepetkin (2001), Open boundary condition for long-term integration of regional oceanic models, *Ocean Modell. 3*, 20 pp., doi:10.1016/S1463-5003(00)00013-5, Hooke Inst. Oxford Univ., Oxford, U. K.

Nitanni, H. (1972), Beginning of the Kuroshio, in *Kuroshio—Its Physical Aspects*, edited by H. Stommel and Y. Yoshida, pp. 129–163, Tokyo Univ. Press, Tokyo.

Pedlosky, J. (1979), *Geophysical Fluid Dynamics*, Springer, New York.

Pedlosky, J. (1996), *Ocean Circulation Theory*, Springer, New York.

Qiu, B., and N. Imasato (1990), A numerical study on the formation of the Kuroshio countercurrent and the Kuroshio Branch Current in the East China Sea, *Cont. Shelf Res.*, *10*, 165–184, doi:10.1016/0278-4343(90)90028-K.

Shchepetkin, A., and J. C. McWilliams (2005), The regional oceanic modeling system: A split-explicit, free-surface, topography-following-coordinate ocean model, *Ocean Modell. 9*, 347–404, doi:10.1016/j.ocemod.2004.08.002.

Song, Y., and D. B. Haidvogel (1994), A semi-implicit ocean circulation model using a generalized topography-following coordinate system, *J. Comput. Phys.*, *115*, 228–244, doi:10.1006/jcph.1994.1189.

Su, J. L., and Y. Q. Pan (1987), On the shelf circulation north of Taiwan, *Acta Oceanol. Sin.*, *6*, suppl. I, 1–20.

Su, Y. S., and X. C. Wong (1994), Water masses in China seas, in *Oceanology of China Seas*, vol. 1, edited by D. Zhou et al., pp. 3–6, Kluwer Acad., Dordrecht, Netherlands.

Su, J. L., Y. Q. Pan, and X. S. Liang (1994), Kuroshio intrusion and Taiwan Warm Current, in *Oceanology of China Seas*, vol. 1, edited by D. Zhou et al., pp. 59–70, Kluwer Acad., Dordrecht, Netherlands.

Takikawa, T., J.-H. Yoon, and K.-D. Cho (2005), The Tsushima Warm Current through Tsushima straits estimated from ferryboat ADCP data, *J. Phys. Oceanogr.*, *35*, 1154–1168, doi:10.1175/JPO2742.1.

Tang, T. Y., J. H. Tai, and Y. J. Yang (2000), The flow pattern north of Taiwan and migration of the Kuroshio, *Cont. Shelf Res.*, *20*, 349–371, doi:10.1016/S0278-4343(99)00076-X.

Teague, W. J., G. A. Jacobs, D. S. Ko, T. Y. Tang, K. I. Chang, and M.-S. Suk (2003), Connectivity of the Taiwan, Cheju, and Korea straits, *Cont. Shelf Res.*, *23*, 63–77, doi:10.1016/S0278-4343(02)00150-4.

Teague, W. J., P. A. Hwang, G. A. Jacobs, J. W. Book, and H. T. Perkins (2005), Transport variability across the Korea/Tsushima Strait and the Tsushima Island Wake, *Deep Sea Res. Part II*, *52*, 1784–1801, doi:10.1016/j.dsr2.2003.07.021.

Wang, Y. H., S. Jan, and D. P. Wang (2003), Transports and tidal current estimates in the Taiwan Strait from shipboard ADCP observations (1999–2001), *Estuarine Coastal Shelf Sci.*, *57*, 193–199, doi:10.1016/S0272-7714(02)00344-X.

Wu, C.-R., H.-F. Lu, and S.-Y. Chao (2008), A numerical study on the formation of upwelling off northeast Taiwan, *J. Geophys. Res.*, *113*, C08025, doi:10.1029/2007JC004697.

Zhang, J., S. M. Liu, J. L. Ren, Y. Wu, and G. L. Zhang (2007), Nutrient gradients from the eutrophic Changjiang (Yangtze River) Estuary to the oligotrophic Kuroshio waters and reevaluation of budgets for the East China Sea shelf, *Prog. Oceanogr.*, *74*, 449–478, doi:10.1016/j.pocean.2007.04.019.

Zhao, B. R., G. F. Ren, D. M. Cao, and Y. L. Yang (2001), Characteristics of the ecological environment in upwelling area adjacent to the Changjiang River estuary, *Oceanol. Limnol. Sin.*, *32*, 327–333.

X. Feng, Z. Liu, D. Yang (corresponding author), and B. Yin, Key Laboratory of Ocean Circulation and Waves, Institute of Oceanology, Chinese Academy of Sciences, 7 Nanhai Rd., Qingdao 266071, China. (yangdezhou@qdio.ac.cn)